High-end chlorophyll fluorescence analysis with the MULTI-COLOR-PAM.
I. Various light qualities and their applications.

Ulrich Schreiber, Christof Klughammer and Jörg Kolbowski

Abstract

The MULTI-COLOR-PAM Multiple Excitation Wavelength Chlorophyll Fluorescence Analyzer is unique in providing 6 different wavelengths of pulse-modulated measuring light, ML (400, 440, 480, 540, 590 and 625 nm), as well as 6 different wavelengths of actinic light, namely 440, 480, 540, 590, 625 and 420-640 nm (white). The variously colored actinic light can be used for continuous illumination (AL), maximal intensity single turnover pulses (ST), high intensity multiple turnover pulses (MT) and Saturation Pulses (SP). In addition, far-red light (FR, peaking at 725 nm) is provided for preferential excitation of PS I. This article outlines the properties and applications of the various colors of measuring and actinic light provided by the MULTI-COLOR-PAM. The pulse-modulated ML can be applied with vastly different pulse frequencies ranging between 10 to 200000 Hz, thus enabling continuous monitoring of quasi-dark fluorescence yield (Fo) as well as measurement of fast induction kinetics in the sub-ms time range using the same ML of various colors. Analysis of the $O-I_1$ fluorescence rise kinetics in saturating light allows determination of the wavelength and sample specific functional absorption cross-section of PS II, $Sigma(II)_\lambda$, with which the PS II turnover rate at a given incident PAR can be calculated. Vastly different light response curves can be obtained with AL of different colors. Based on $Sigma(II)_\lambda$ the usual PAR, in units of µmol quanta/(m² · s), can be converted into PAR(II), in units of PS II effective quanta/s, in order to compare the responses obtained with differently colored AL. A fluorescence-based electron transport rate $ETR(II) = PAR(II) \cdot Y(II)/Y(II)_{max}$ is defined, which in contrast to the usual relative ETR can describe the rate of electron transport even in dilute suspensions of unicellular algae and cyanobacteria. When chlorophyll content is known, an absolute rate of O_2 evolution can be estimated from ETR(II). The MULTI-COLOR-PAM is also well suited for measurements with leaves, for which a special optical unit with clip-holder is provided. For this application the use of 440 nm ML/AL/ST/MT/SP and detection of F < 710 nm are recommended.

1   Introduction

1.1   Unique features of the MULTI-COLOR-PAM

The MULTI-COLOR-PAM is founded on the tradition of previous Pulse-Amplitude-Modulation (PAM) chlorophyll fluorometers, i.e. mainly the PAM-100, XE-PAM, PHYTO-PAM, DUAL-PAM-100 and PAM-2500. It now combines virtues of these proven instruments in one compact device and in addition offers a number of unique properties, rendering it the high-end choice for chlorophyll fluorescence analysis. It is not only suited for reliable routine measurements, like assessment of effective PS II quantum yield, non-photochemical quenching and relative electron transport rate, but also for sophisticated work on special aspects of photosynthesis, like wavelength dependence of electron transport rate, reversible state 1-state 2 transitions and changes of absorption cross-section of PS II.

At the core of the MULTI-COLOR-PAM is a multi-color Chip-on-Board (COB) LED Array specially developed for this particular purpose in cooperation with PerkinElmer Elcos GmbH (Pfaffenhofen, Germany) and a dedicated microprocessor-based controller for its light-output and the processing of the fluorescence responses. Special user friendly software is provided for recording and analyzing the data.

The multi-color COB-Array consists of 60 Power-LED-chips on a 10 x 10 mm area, featuring a total of 8 different colors, which are randomly mixed by a 10 x 10 mm *Perspex* light pipe. This leads to a 10 x 10 mm glass cuvette in the optical unit, in which the suspended sample can be stirred continuously. For leaf measurements an optional optical unit is provided, featuring a pyramidal *Perspex* light pipe (base 10 x 10 mm, top 6 x 6 mm) and a clip-holder.

In conjunction with the dedicated user-software, this set-up provides the means for creating a unique variety of different light qualities in terms of colors, intensities, pulse-forms and pulse-frequencies. Default settings and automated measuring routines are provided for standard measurements that have proven useful for basic chlorophyll fluorescence analysis. For advanced studies the MULTI-COLOR-PAM offers numerous possibilities of user-defined illumination protocols. In this respect, the MULTI-COLOR-PAM resembles a sophisticated music

instrument, like an organ with numerous "registrations", the performance of which depends on the skill and imagination of the player.

The MULTI-COLOR-PAM is unique in combining the information obtained from fast kinetic measurements in the sub-ms time range with steady-state information obtained e.g. with the help of light response curves. In particular, reliable assessment of the wavelength-dependent absorption cross-section of PS II, Sigma (II), opens the way for profound fluorescence-based analysis of photosynthetic electron transport and its regulation in variously pigmented organisms.

The many different aspects and applications of the MULTI-COLOR-PAM will be outlined in a series of PAM Application Note (PAN) articles. The present article deals with the different light qualities and their applications. A separate article will be dedicated to far-red light, of which a wide range of intensities is provided for preferential excitation of PS I. Particular emphasis is put on the fact that light responses of photosynthetic organisms essentially depend on light color. To take account of this color-specific behavior, the usual scale of wavelength-independent photosynthetically active radiation (PAR scale) needs to be transformed into a PS II-specific, wavelength-dependent "PAR(II) scale". The MULTI-COLOR-PAM is unique in providing the means for transformation of the original PAR scale into a PAR(II) scale.

1.2 Pulse-modulated measuring light vs. actinic light

For understanding PAM fluorimetry in general and the MULTI-COLOR-PAM in particular, it is important to rationalize the difference between measuring light (ML) and actinic light (AL). The ML is pulse-modulated, i.e. consisting of µs light pulses applied at defined frequencies (i.e. with defined periodical dark intervals), which excite corresponding fluorescence pulses that are selectively amplified by a synchronized amplifier. The AL is not pulse-modulated and, hence, neither the signal caused by the AL as such nor the AL-excited fluorescence are processed by the selective amplifier system.

Generally speaking, all types of light that change the state of the photosynthetic apparatus have an "actinic effect". In principle, this is also true for the pulse-modulated ML, if this is applied at sufficiently high intensity and pulse frequency. The MULTI-COLOR-PAM provides very strong ML pulses which, depending on pulse frequency, can have practically no or a rather strong actinic effect (see section on ML below).

In addition, there are special types of actinic illumination, that are single and multiple turnover flashes, which rapidly close PS II reaction centers. In the PAM literature, however, AL normally stands for continuous illumination that serves for driving a continuous photosynthetic electron flow. "Saturating single turnover flashes" (ST) are applied to close all PS II reaction centers within a time shorter than the dark-reoxidation of the primary PS II acceptor. "Multiple turnover flashes" (MT) are used to reduce not only the primary acceptor Q_A, but also the secondary plastoquinone (PQ) acceptor pool. "Saturating multiple turnover flashes", also called "Saturation Pulses" (SP), have routinely been applied with PAM fluorimeters for SP-analysis of chlorophyll fluorescence, yielding a variety of fluorescence based parameters, including effective PS II quantum yield, Y(II), maximal PS II quantum yield, Fv/Fm = Y(II)max, and non-photochemical quenching, NPQ.

The MULTI-COLOR-PAM offers the possibility to choose between different colors of ML, AL, ST and MT/SP. This possibility is particularly important for work with organisms that display a particular antenna pigment composition or for the study of wavelength dependent processes, as e.g. reversible state transitions and orange carotenoid protein (OCP) quenching. While on first sight the color aspect may appear to apply only to algae and cyanobacteria, it is also important for leaf studies. As recently emphasized by Rappaport et al. (2007), the actual fluorescence information from leaves is highly dependent on the depth of light penetration into the leaf, which again is determined by the light color.
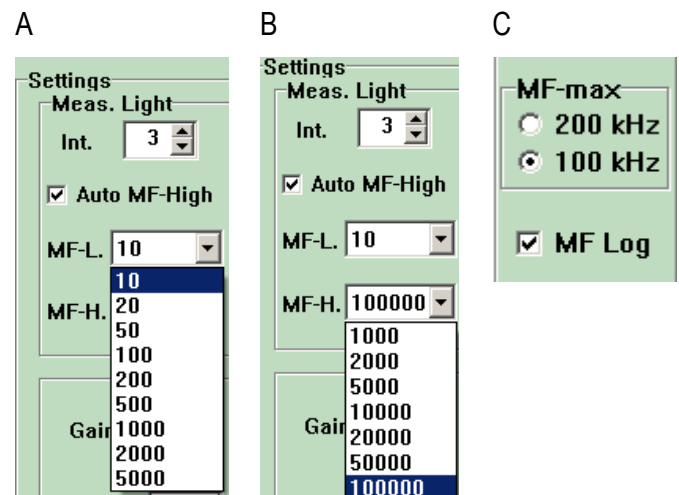

Figure 1. Measuring light settings.

2 Properties of the different types of light provided by the MULTI-COLOR-PAM

2.1 Measuring light, ML

The MULTI-COLOR-PAM provides pulse-modulated ML with peak-wavelengths at 400 nm (dark-violet), 440 nm (blue-violet), 480 nm (cyan-blue), 540 nm (green), 590 nm (orange) and 625 nm (red-orange). Spurious ML at wavelengths above 640 nm is eliminated by a short-pass interference filter, so that the photodiode detector, which is protected by a long-pass filter (> 650 nm), will not see any ML directly, but only the pulse-modulated fluorescence (peak emission at 685 nm) that is excited by the ML.

Table 1. Properties of the ML-part of the multi-color LED array. The PAR values apply for ML intensity setting 10 (ML10) and 100 kHz ML pulse frequency (MF 100K).

Peak wavelength, nm	400	440	480	540	590	625
Color						
Number of LED chips on COB	1	4	3	8	8	6
PAR at output of *Perspex* rod $\left[\dfrac{\mu E}{m^2 \cdot s}\right]$	26	468	618	403	198	318

An individual ML-pulse has a width of 1 μs, which even at maximal LED-current (i.e. maximal setting of ML-intensity) does not cause any appreciable closure of PS II reaction centers. In principle, this remains true also when ML-pulses are applied repetitively (pulse-modulation), as long as Q_A^- cannot accumulate, i.e. the dark-time between individual ML-pulses is sufficiently long for reoxidation of Q_A^- by the secondary PS II acceptor Q_B and the PQ-pool. There is, however, a type of variable fluorescence, which can be induced at extremely low light intensities, thus simulating a population of PS II centers inactive in secondary electron transport (Chylla et al. 1987, Lavergne and Leci 1993). The MULTI-COLOR-PAM is well-suited for studying the properties of such "inactive" PS II centers, which will be dealt with in a separate PAN communication.

For each ML color the user may choose between 20 different intensity settings and 13 different pulse-frequency settings, which cover the range from 10 Hz to 100 kHz (i.e. factor of 10^4; cf. Fig. 1). For fast kinetics recordings, even a maximal pulse frequency (MF-max) of 200 kHz can be selected. A low frequency setting (MF-L) is used for quasi-dark assessment of Fo, i.e. of the minimal fluorescence yield observed when all PS II reaction centers are open. At the same time, a high frequency setting (MF-H) can be pre-selected, which becomes effective only when the actinic light is switched on and the "Auto MF-H function" is enabled. Hence, for the sake of a high signal/noise ratio, relatively strong ML-pulses can be used, which at MF-L have a negligibly small actinic effect. Upon automatically switching to MF-H, the light-induced changes of fluorescence yield are measured with high time resolution.

Measurements of relaxation kinetics (e.g. reflecting Q_A^- reoxidation following a saturating single turnover flash) demand on the one hand maximal MF for resolving the initial rate in the sub-ms time range and on the other hand low MF for resolving slow decay components under quasi-dark conditions. For this application a special "MF Log mode" is provided (under Fast Settings; cf. Fig. 1), which is initiated simultaneously with MF-max being turned off, resulting in logarithmically decreasing MF.

The relative intensities of the various ML colors differ considerably from each other. They are determined by the particular LED chip material and the number of chips on the COB-LED-array. At a given color, the effective ML-intensity is determined by the selected measuring light intensity and pulse-frequency.

At MF-H the contribution of the ML to overall actinic intensity can be considerable. The software accounts for this contribution when displaying the quantum flux density of photosynthetically active radiation (PAR). Table 1 shows, for the 6 different ML-wavelengths, the number of chips on the COB-LED-Array and the PAR at the exit of the 10 x 10 mm *Perspex* light guide. The intensity values show some variation between individual instruments, and for quantitative work they have to be measured with a suitable quantum sensor (like US-SQS/B or MQS-B, Walz).

The differences in PAR output of the variously colored chips are partially counterbalanced by the number of chips used. For example, the 480 nm ML features 3 chips only, as these chips are particularly powerful, whereas the 590 nm ML employs 8 chips, the light output of which is an order of magnitude lower than that of blue chips (cf. Table 1). The intensity of the 400 nm ML on purpose is much weaker than that of the other ML colors, as this ML wavelength is primarily provided for special applications like assessment of "yellow substances" (humic acids, gilvin) in natural waters. The same multi-color-COB is also employed in the new PHYTO-PAM phytoplankton analyzer, where this aspect is quite important. The 480 nm ML displays the highest PAR. At 100 kHz and ML 10 the resulting 618 μmol quanta/(m² · s) is equivalent to relatively strong actinic light, which, e.g. in green algae, may even saturate photosynthetic electron flow. At 10 Hz, however, the time-integrated PAR only amounts to 0.0618 μmol quanta/(m² · s) , the actinic effect of which can normally be neglected.

Except for the 400 nm ML, the various colors of ML and AL, ST and MT/SP are generated by the same type of LED-chips. Therefore, when the same colors of ML and AL are selected, the actinic effects of both types of light are fully equivalent and correspondingly taken into account by the software (e.g. in the display of light response curves).

2.2 Wavelength-dependence of normalized Fo/PAR and absorptance

Low ML-frequency (MF-L) is used to assess the quasi-dark level of fluorescence yield, Fo, the amplitude of which depends on the color of the ML as well as on the antenna pigment composition and content of the investigated organism.

In Table 2 and Fig. 2, the Fo values measured with 440, 480, 540, 590 and 625 nm ML in dilute suspensions of green algae (*Chlorella vulgaris*) and cyanobacteria (*Synechocystis* PCC 6403) are compared using identical settings of ML-intensity and Gain (signal amplification). The cell densities in the two suspensions were adjusted to give the same absorptance at 440 nm (see below). At the applied ML intensity setting (ML 5) and minimal pulse-frequency (MF-L 10), the effective intensities of the incident PAR generally are too low to induce any fluorescence increase beyond Fo (even with respect to "inactive PS II").

The relative PAR-values of the differently colored ML are important for interpretation of the Fo information in terms of PS II excitation. The PAR-scaled Fo levels (i.e. Fo/PAR) measured with various ML-colors provide the equivalent of an approximate 5-point fluorescence excitation spectrum (see Fig. 2). The Fo/PAR data were normalized to 1 relative unit at the maximal signal value, which was observed with *Synechocystis* and 625 nm excitation.

The wavelength-dependence of dark-fluorescence yield, Fo, differs considerably between *Chlorella* and *Synechocystis*. Despite the identical absorptance at 440 nm, i.e. although the same fraction of incident 440 nm quanta is absorbed in the *Chlorella* and *Synechocystis* suspensions, the Fo(*Chlorella*)$_{440}$ exceeds the Fo(*Synechocystis*)$_{440}$ by a factor of 2.294/0.359 = 6.4. In contrast, when 625 nm excitation is used with the same samples, which in cyanobacteria is strongly absorbed by phycocyanin, the Fo(*Synechocystis*)$_{625}$ exceeds the Fo(*Chlorella*)$_{625}$ by a factor of 1.702/0.522=3.3.

Table 2. Comparison of Fo and PAR-scaled Fo (Fo/PAR) of dilute suspensions of *Chlorella* and *Synechocystis* measured with 5 different colors at identical settings of ML-intensity (ML 5) and minimal pulse-frequency (MF-L 10). The Fo/PAR values were normalized to give 1 rel. unit at 625 nm with *Synechocystis*, where the maximal signal was obtained.

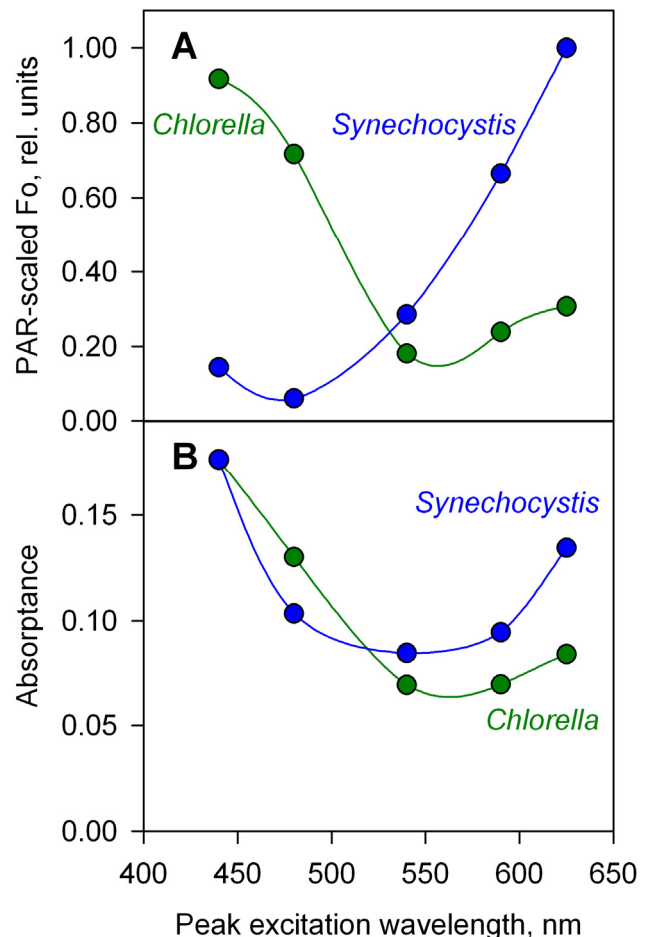| Parameter	Unit					
Peak wavelength of ML	nm	440	480	540	590	625
Incident PAR	$\frac{\mu mol}{m^2 \cdot s}$	0.0234	0.0309	0.0201	0.0099	0.0159
Incident PAR	rel. units	75.7	100.0	65.2	32.0	51.5
Fo(*Chlorella*)$_\lambda$	Volt	2.294	2.366	0.389	0.252	0.522
$\frac{Fo(Chlorella)_\lambda}{PAR}$	rel. units	0.917	0.716	0.181	0.238	0.307
Fo(*Synechocystis*)$_\lambda$	Volt	0.359	0.198	0.616	0.703	1.702
$\frac{Fo(Synechocystis)_\lambda}{PAR}$	rel. units	0.143	0.060	0.286	0.665	1.000

Figure 2.

A: Comparison of normalized Fo/PAR in dilute suspensions of *Chlorella* and *Synechocystis*. The data were normalized to unity at maximal relative Fo/PAR, i.e. 625 nm with *Synechocystis*.

B: Comparison of absorptance in the same suspensions of *Chlorella* and *Synechocystis*, the PAR-scaled Fo data of which are compared in A. Cell densities of the two suspensions were adjusted to give the same absorptance at 440 nm.

The Fo/PAR plots of *Chlorella* and *Synechocystis* in Fig. 2A can be compared with the corresponding absorptance spectra in Fig. 2B, measured with the MULTI-COLOR-PAM under identical optical conditions.

The MULTI-COLOR-PAM allows a determination of the wavelength-dependent absorptance of the same sample in which chlorophyll fluorescence is measured using the standard Optical Unit ED-101US. For this purpose, the detector-unit has to be moved from the 90° position (relative to the emitter-unit) to the 180° position, which just takes a couple of minutes. The long-pass filter in front of the detector has to be exchanged against a suitable neutral density filter (or pin-hole diaphragm), so that the pulse-modulated transmittance signals can be measured both with the suspension medium, I_1(medium), and with the sample I_1(sample). The absorptance a (=1-transmittance) is calculated as follows:
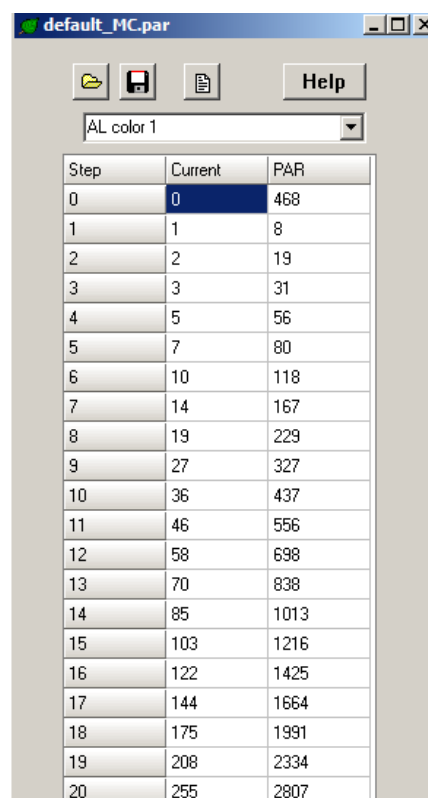
$$a = 1 - \frac{I_1(\text{sample})}{I_1(\text{medium})} \tag{1}$$

While the spectra of Fo/PAR and absorptance resemble each other with *Chlorella*, they differ considerably in the case of *Synechocystis*. This is due to the fact that chlorophyll fluorescence originates mainly from PS II and that the difference in pigment composition between PS I and PS II is much larger in *Synechocystis* than in *Chlorella*. In cyanobacteria, most of the Chl *a* is contained in the PS I antenna, whereas the phycobilisomes constitute the main PS II antenna system. Comparison of the Fo/PAR and absorptance data show that measurements of wavelength dependent fluorescence provides complementary information on PS II absorption, which cannot be obtained from absorptance data, as besides PS I pigments also other pigments and constituents contribute to overall light absorption. As will be shown below, the most specific information on PS II absorption is provided by measurements and analysis of the fast fluorescence rise upon onset of high intensity illumination of different colors (see section 3.2).

2.3   Actinic light, AL

The MULTI-COLOR-PAM provides continuous AL with the same wavelengths as provided for ML, except for the 400 nm AL (see Table 1 and text above). In addition, also white actinic light (420-640 nm) is provided. Wavelengths above 640 nm are eliminated by a short-pass interference filter, so that the photodiode detector, which is protected by a long-pass filter (> 650 nm), does not see any AL directly, but only the non-modulated fluorescence (peak emission at 685 nm) that is excited by AL. Non-modulated fluorescence, however, is not processed by the PAM amplifier system, which selectively amplifies the pulse-modulated signal. Actinic light generally serves for driving photosynthetic electron transport by charge separation at the reaction centers of PS I and PS II. As already mentioned above, in PAM applications the term AL is mostly used for continuous actinic light,

whereas very short pulses (up to 50 µs width) of very strong actinic light are referred to as "single turnover flashes" (ST) and strong longer pulses (up to about 800 ms) are called "multiple turnover flashes" (MT) or "saturation pulses" (SP). These special types of actinic illumination will be dealt with in separate sections below. The same applies to far-red actinic light (FR), which is preferentially absorbed by PS I, which will be dealt with in a separate PAN-article.
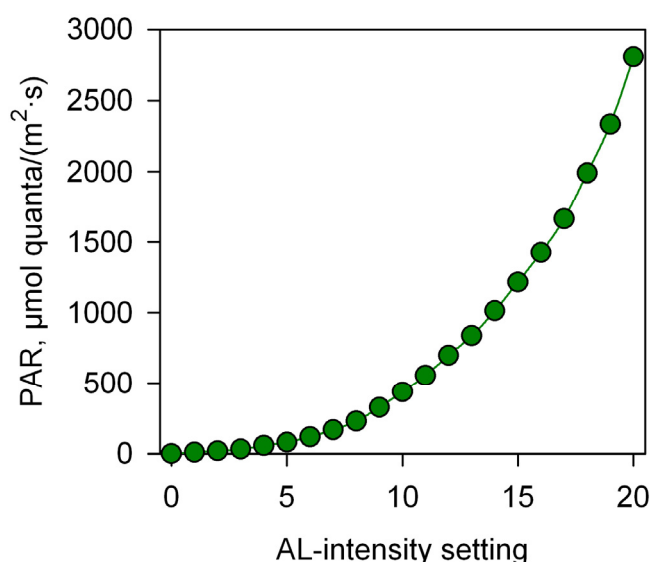

Figure 3. Upper panel: Screenshot of default PAR list for 440 nm. Left column, intensity settings. Center column, relative current values. Right column, PAR values in µmol quanta/(m² · s). Lower panel: PAR values in µmol quanta/(m² · s) as a function of AL-intensity setting for one of six AL-colors (AL color #1, 440 nm) as defined by the default current/PAR list for suspensions (default_MC.par).

Table 3. Properties of the AL-part of the multi-color LED array. The PAR values apply for maximal AL intensity setting 20 (AL 20).

Peak wavelength, nm	440	480	540	590	625	420-645
Color						
Number of LED chips on COB	4	3	8	8	4	2
Maximum PAR at output of *Perspex* rod $\left[\frac{\mu E}{m^2 \cdot s}\right]$	2807	3907	4724	1758	2250	4936

For each color the user may choose between 20 intensity settings, corresponding to defined LED currents and PAR values at the exit of the *Perspex* light guide of the emitter unit. For standard applications default current/PAR lists with progressively increasing intensity settings are provided (default_MC.par for suspensions and default_leaf.par for leaves). The default lists can be readily modified by the user and saved in new par-files. LED current can be adjusted in 255 steps. The PAR defined in the default lists were measured with the spherical quantum sensor US-SQS/B and the planar sensor MQS-B for suspensions and leaves, respectively (Heinz Walz GmbH). These sensors can be directly connected to the Ext.Sensor input of the MULTI-COLOR-PAM Power-and-Control unit. A special routine is provided for automated measurements of PAR-lists. Most importantly, the PAR-signals are processed with high time resolution, so that even the intensities of MT pulses in the ms time range are reliably assessed.

As already pointed out in the section on measuring light (ML), the ML may contribute significantly to overall PAR, if applied at high pulse frequency. Based on the given information on presently effective ML-intensity and ML-frequency settings, the corresponding PAR is calculated by the PamWin program and taken into account in the PAR display.

In the PAR list, the PAR-value for AL-intensity setting 0 corresponds to ML of the same color at ML Int. setting 10 and MF 100 kHz. It is assumed that the PAR contributed by the ML is proportional to ML-intensity and ML-frequency. The screenshot in Fig. 3 (top) shows the default PAR-list for AL-color #1 (440 nm). In the bottom panel the corresponding plot of the PAR in µmol quanta/(m² · s) vs. the AL-intensity settings is displayed.

Table 3 shows for the 6 different AL-colors the number of chips on the COB-LED-Array and the PAR at the exit of the 10 x 10 mm *Perspex* light guide for the maximal AL intensity setting 20 (AL 20). In practice, the overall PAR is somewhat increased by the PAR contribution of the ML at high pulse-frequency, which is taken into account. For all measurements the overall PAR calculated according to the current PAR list is saved together with the fluorescence data.
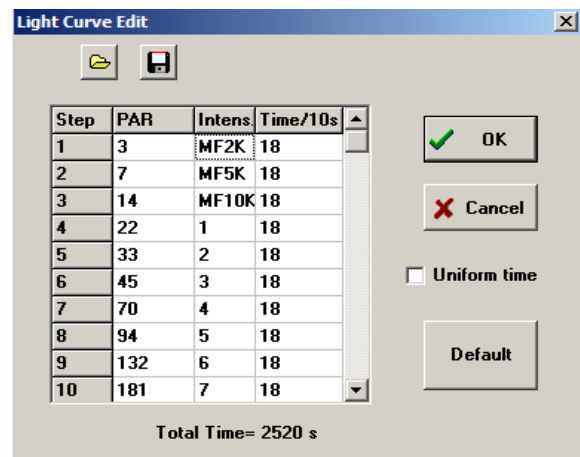

Figure 4. Screenshot of "Light Curve Edit" window. Left-most column, illumination step of light treatment. Second column from left, PAR values in µmol quanta/(m² · s). Third column from left, intensity setting. Right-most column, width of illumination step (here 180 s for all steps).

The PAR output per chip differs considerably for the various colors, which to some extent is balanced by the number of chips. While white AL yields the highest PAR, its role differs from that of the other colors, as no white ML is provided and, hence, depending on the choice of ML-color, ML-intensity and ML-frequency, the spectral composition of the overall actinic illumination will vary, when white AL is selected. With green organisms, in conjunction with white AL the use of green ML may be recommended, as this contributes only marginally to the overall actinic effect. The white LED chips contribute significantly to the overall intensity of saturating ST flashes (see section below), where spectral composition is not important, as long as saturation is reached.

While normally the same color is used for ML and AL, it is also possible to select different colors. For example, in the study of cyanobacteria, Chl *a* fluorescence can be directly excited by weak 440 nm ML absorbed by Chl *a* in the thylakoid membrane, whereas electron transport can be driven by 625 nm AL absorbed within the phycobilisomes. In this way, important information on reversible state 1-state 2 transitions can be obtained. Examples of such measurements will be presented in a separate PAN article.

AL is used routinely for measurements of dark-light induction kinetics (Kautsky effect) and for light response curves (Light Curves). For these applications, the PamWin user surface provides the "Slow Kinetics", "Fast Kinetics" and "Light Curve" windows, as well as a number of automated measuring routines. In all these measurements the AL-induced responses depend not only on the PAR, but also on the color of the applied AL and the pigment composition of the investigated sample. Hence, for quantitative work, not only the knowledge of PAR is essential, but also of the wavelength-dependent functional cross-section of the investigated sample.

As *in vivo* fluorescence yield primarily reflects the efficiency of charge separation at PS II reaction centers, the absorption of AL by PS II is essential. It differs for various colors and organisms. For example, a given PAR of blue light will elicit a strong response in green algae, whereas the same light induces a weak response in cyanobacteria. Conversely, a given PAR of short-wavelength red light (625 nm) may induce a strong effect in cyanobacteria, while a relatively weak response is observed in green algae. This aspect will be elaborated on in the following chapter 3.

3   Applications, calculations and definitions

3.1   Wavelength dependent Light Curves and relative electron transport rates (ETR)

The light response of photosynthetic organisms routinely is analyzed with the help of fluorescence-based Light Curves (LC), consisting of a number of illumination steps with increasing intensities of photosynthetically active radiation, PAR. The MULTI-COLOR-PAM is ideally suited for measuring LC with outstanding accuracy even at rather low chlorophyll content, with the advantage of avoiding light intensity gradients. The number of LC steps, as well as the widths and intensities of the individual steps can be programmed by the user.
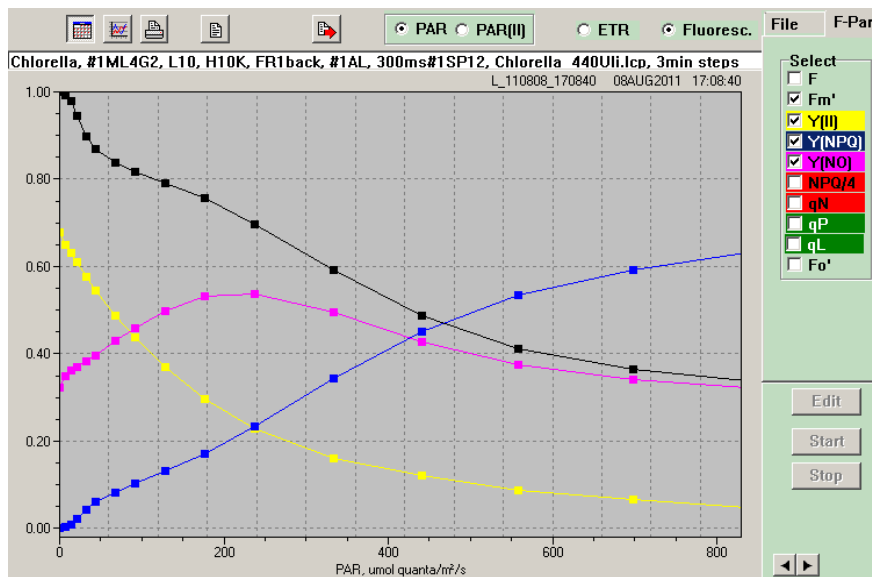

Figure 5. Typical Light Curves of Fm' and of the derived complementary PS II quantum yields Y(II), Y(NPQ) and Y(NO) measured with dilute *Chlorella* suspension (300 µg Chl/L) using the MULTI-COLOR-PAM with 440 nm light.
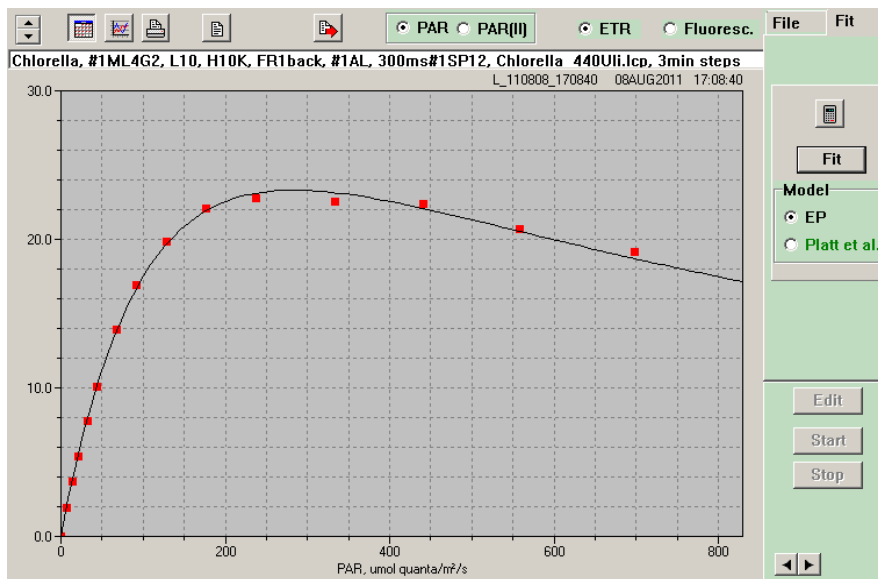

Figure 6. Typical Light Curve of relative ETR measured with dilute *Chlorella* suspension (300 µg Chl/L) using the MULTI-COLOR-PAM with 440 nm light and a default ETR-factor of 0.42.
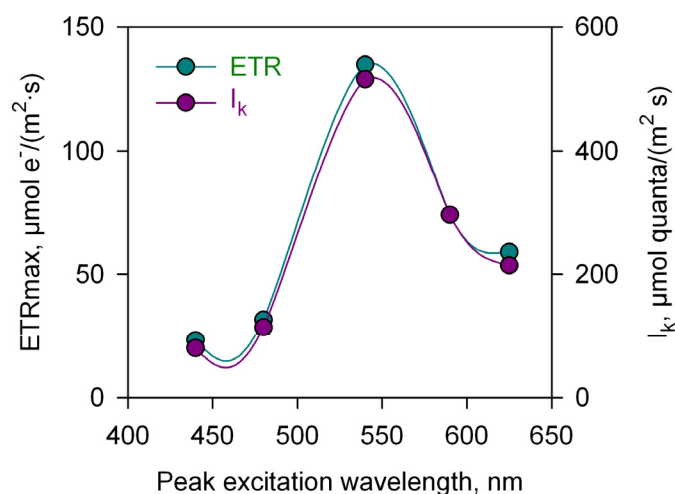
Wavelength, nm	α	ETRmax	I_k
440	0.292	23.3	79.8
480	0.277	31.6	114.1
540	0.262	134.8	515.3
590	0.250	73.9	295.7
625	0.275	58.9	214.2

Figure 7. ETRmax and I_k values of *Chlorella* plotted against the peak wavelength of the AL. Relative ETR light curves were measured with same *Chlorella* sample using different AL colors and a default ETR-factor of 0.42. Parameters were estimated according to the model of Eilers and Peeters (1988). The original relative ETR light curve with 440 nm AL is shown in Fig. 6. The table lists plotted data (ETRmax and I_k) and α.

As the spectral properties of the ML are identical to those of the AL (provided the same color is selected), ML at high ML-Frequency (MF 2K etc.) can be used for covering the low PAR range (see Fig. 4).

The illumination time periods (step widths) at the various PAR may vary between 10 s (resulting in so-called "rapid light curves", RLC) and many minutes. The longer the illumination steps, the more fluorescence based LC approach classical P vs. E curves (photosynthesis versus irradiance curves), where steady state is reached within each PAR-step, before photosynthetic rate is evaluated.

Figures 5 and 6 show screen shots of LC-data measured with a dilute suspension of *Chlorella* (300µg Chl/L) using 440 nm light and 3 min illumination steps. In the example of Fig. 5 the fluorescence based complementary PS II quantum yields of photochemical energy conversion, Y(II), regulated non-photochemical energy conversion, Y(NPQ), and non-regulated non-photochemical energy loss, Y(NO) are selected for display together with the original Fm' data obtained with the help of Saturation Pulses (SP). These parameters provide basic information on the fate of absorbed light energy (Kramer et al. 2004, Klughammer and Schreiber 2008).

While a detailed discussion of the present data would be beyond the scope of the present application note, the pronounced biphasic PAR-dependence of Y(NPQ) may be pointed out, which to some extent also affects Y(II). The biphasic character does not disappear with longer illumination steps (data not shown), i.e. it does not seem to be related to an induction effect. Based on the Y(II) data, relative electron transport data (rel. ETR) can be calculated and plotted vs. PAR (see Fig. 6).

Relative electron transport rate (rel. ETR) as a fluorescence-derived parameter was introduced for PAM-measurements with leaves (Schreiber et al. 1994):

$$\text{rel. ETR} = Y(II) \cdot PAR \cdot \text{ETR–factor} \qquad (2)$$

(While formally units of µmol electrons/(m² · s) apply for rel. ETR, in practice normally "rel. units" are used).

The ETR-factor is supposed to account for the fraction of overall incident PAR that is absorbed within PS II. In most published studies, however, no attempts were made to determine the ETR-factor, which simply has been assumed to correspond to that of a "model leaf", with 50% of the PAR being distributed to PS II and 84% of the PAR being absorbed by photosynthetic pigments in a standard leaf (Björkman and Demmig 1987), so that normally a default ETR-factor of 0.42 is applied.

Without detailed knowledge of the true PS II specific absorbance, ETR can give a rough estimate only of relative photosynthetic electron transport rate. In the case of dilute algae suspensions, where a minor part of overall incident radiation is absorbed, normally rel. ETR is just treated as an intrinsic parameter of *relative* rate of PS II turnover without any information on *absolute* rate, calculation of which would require information on PS II content and the functional absorption cross-section of PS II (see sections 3.2 and 3.3).

Attempts of fluorescence-based determination of *absolute* rates of PS II turnover in algal suspensions so far have been the exception (see e.g. Gilbert et al. 2000a, Jakob et al. 2005). For calculation of absolute rates, the absorbed photosynthetic radiation (Q_{phar}) has been estimated from algal absorption spectra and the emission spectrum of the applied light source (Gilbert et al. 2000b). This approach, however, is based on the overall absorption of the sample, whereas for proper evaluation of fluorescence data the specific PS II absorption is decisive.

In the measurement of rel. ETR data presented in Fig. 6, no attempt was made to obtain absolute rates and the default value of 0.42 was applied as ETR-factor. With this kind of approach, rel. ETR is independent of Chl content, just like Y(II), from which it is derived and, hence, essentially describes the relative frequency of charge separa-

tion at PS II reaction centers. Thus defined light curves of rel. ETR provide useful information, as long as the performance of a particular organism is studied using a fixed color of light, as is the case with standard PAM fluorometers. For this purpose, standard PAM-software provides routines for fitting the LC-parameters α, ETRmax and I_k using models developed by Eilers and Peeters (1988) or Platt et al. (1980). The parameter α relates to the maximal PS II quantum yield (initial slope of LC). ETRmax is a measure of maximal relative rate and I_k relates to the PAR at which light saturation sets in (defined by ETRmax/α).

The values of these Light Curve parameters are strongly dependent on the color of light and PS II absorption of the sample. Hence, when LC are measured with the MULTI-COLOR-PAM using different AL-colors, vastly different ETRmax and I_k values are obtained for the same sample, (Fig. 7). Notably, in *Chlorella* there are even considerable differences between the two types of blue light (440 and 480 nm) and red light (625 nm). These data show that the same quantum flux density of differently colored light within the range of "photosynthetically active radiation", PAR, can have vastly different outcomes, not only between differently pigmented organisms, but also within the same organism.

ETRmax and I_k display very similar wavelength dependency, in the case of *Chlorella* with peak and minimal values at 440 and 540 nm, respectively. The ETRmax and I_k spectra resemble inverse Fo/PAR spectra (see Fig. 2). It should be kept in mind, however, that PS I contributes to Fo, and that ETRmax as well as I_k are not only dependent on PS II but also on PS I activity.

The MULTI-COLOR-PAM has opened the way for detailed studies of electron transport as a function of the color of radiation in photosynthetic organisms with largely different pigment composition. From the data in Fig. 7 it is obvious that in order to make full use of this new potential of the MULTI-COLOR-PAM, either a wavelength- and sample-dependent ETR-factor has to be defined or the quantum flux density of photosynthetically active radiation, PAR, has to be replaced by a PS II specific quantum flux rate, PAR(II). The latter approach is advantageous, as it results in determination of an absolute rate, independent of chlorophyll content. It requires information on the wavelength- and sample-dependent functional cross-section of PS II, Sigma(II)$_λ$, which can be readily obtained with the MULTI-COLOR-PAM (see section 3.2). As will be outlined in section 3.3, PAR can be transformed into PAR(II) simply by multiplication with a Sigma(II)$_λ$-based factor.

3.2   PAR and wavelength- and sample-dependent functional absorption cross-section of PS II, Sigma(II)$_λ$

The PAR usually is defined for wavelengths between 400-700 nm (Sakshaugh et al. 1997) in units of μmol quanta/(m² · s). It is measured with calibrated quantum sensors, like the spherical US-SQS/B (for suspensions) or the planar MQS-B (for leaves) from WALZ. Such devices measure the overall flux density of incident quanta, without making any distinction between quanta of different colors, as long as their wavelengths fall into the 400 to 700 nm PAR range.

Hence, the actual extent of PAR-absorption (whether by PS II or PS I or any other colored constituents) by the photosynthetically active sample normally is *not* taken into account. While this kind of approach may be feasible in the study of leaves, which display relatively flat absorbance spectra and absorb most of the incident light, it does not work with dilute suspensions of unicellular algae and cyanobacteria, where PS II excitation by light of different wavelengths may vary by an order of magnitude (see data in section 2.2 above) and only a fraction of the incident light is absorbed.

Rappaport et al. (2007) recently pointed out that the "most commonly used unit for light intensity ... μmol of photons s^{-1} m^{-2} … has little experimental value since it cannot reliably be translated into a photochemical rate without knowing the absorbance of the sample, which is rarely the case". Further, the authors note that "there is ... a real need for a more relevant unit which should be the number of electrons transferred per unit time and per PS II reaction center." As will be outlined below, for quantitative work with the MULTI-COLOR-PAM, e.g. analysis of light response curves (LC), we propose the use of PAR(II) instead of PAR, which may serve the purpose suggested by these authors.

In PAM applications, exact information on PAR, measured in units of μmol quanta/(m² · s) with standard quantum sensors *is* very essential, e.g. in conjunction with LC recordings. However, as already outlined in section 3.1, the PAR information has to be complemented with information on the PS II efficiency of the applied PAR with respect to a given sample. Such information is contained in the wavelength-dependent functional cross-section of PS II, the Sigma(II)$_λ$, which depends on both the spectral composition of the applied irradiance (i.e. the AL-color) and the PS II absorption properties of the investigated sample.

The value of Sigma(II)$_λ$ can be derived from the initial rise of fluorescence yield upon onset of saturating light intensity, which directly reflects the rate at which PS II centers are closed. The rate of charge separation of open PS II centers**, k(II),** matches the quantum flux rate of **PS II effective light**, which may be defined as **PAR(II)** (see section 3.3 below). In order to account for the overlapping re-opening of PS II centers by secondary electron transport (reoxidation of Q_A^- by Q_B), either a PS II inhibitor like DCMU has to be added, which is not feasible for *in vivo* studies, or PAR(II) has to be extremely high, so that the reoxidation can be ignored (Kolber et al. 1998; Nedbal et al. 1999; Koblizek et al. 1998), or the rise kinetics have to be corrected for the reoxidation rate.

The latter approach is applied with the MULTI-COLOR-PAM, which will be outlined in detail in a separate PAN article (Klughammer C, Kolbowski J and Schreiber U). Here just one practical example will be given using the same sample (dilute suspension of *Chlorella*) and AL-color (440 nm), with which the Light Curves in Figs. 5-6 were measured.

Figure 8 shows a typical example of the initial part of the increase of fluorescence yield induced by strong AL (in PAM-literature called O-I_1 rise). The O-I_1 rise basically corresponds to the O-J phase of the polyphasic OJIP kinetics that have been described in detail by Strasser and co-workers (for reviews see Strasser et al. 2004, Stirbet and Govindjee 2011). There are, however, essential differences in the measuring techniques and definitions of I_1 and J, which argue for different nomenclatures. The MULTI-COLOR-PAM allows the use of so-called "Fast Trigger Files" for routine measurements of fast kinetics. In the example of Figure 8, the pulse-modulated ML was triggered with 100 kHz pulse-frequency at 100 µs before onset of 440 nm AL.

At 1 ms after onset of AL, a saturating 50 µs multi-color single turnover pulse was applied (see section 4 on single turnover pulse, ST). The ST closes PS II reaction centers transiently so that the so-called I_1-level of fluorescence yield can be determined. The I_1-level corresponds to the maximal fluorescence yield that can be reached in the presence of an oxidized PQ-pool (for apparent PQ-quenching see Samson et al. 1999; Schreiber 2004).

Here, weak far-red (FR) background light is routinely applied in order to assure a fully oxidized PQ-pool, which is particularly important in the study of algae and cyanobacteria. Furthermore, FR-preillumination minimizes the

contribution of "inactive PS II" to the O-I_1 kinetics. Possible artifacts caused by rapid switching of high-intensity non-modulated light is avoided by corresponding gating time periods in the fast trigger files.

At a first approximation, assuming that the AL-driven increase of fluorescence yield is linearly correlated with accumulation of Q_A^-, and that the initial rise is negligibly slowed down by Q_A^- reoxidation, the kinetics can be described by a first order reaction, of which the time constant Tau = 1/k(II) corresponds to the time for reaching a Q_A-reduction level of 100(1-1/e) = 63.2% . When this approximation is applied to the O-I_1 rise of Fig. 8, Tau = 0.379 ms is estimated. A very similar Tau-value (Tau = 0.382 ms) is obtained when the area growth method is applied (details on various fitting routines provided by the MULTI-COLOR-PAM will be presented in an upcoming PAN article).

A thorough analysis of the O-I_1 rise kinetics, however, has to take into account both Q_A^- reoxidation and non-linearity between ΔF and the fraction of reduced Q_A. This can be achieved by a fitting routine we have specially developed for this purpose, which is based on the reversible radical pair model of PS II originally described by Lavergne and Trissl (1995) that was extended to take account of Q_A^--reoxidation (Klughammer C, Kolbowski J and Schreiber U, in preparation).

Variable parameters in this model are

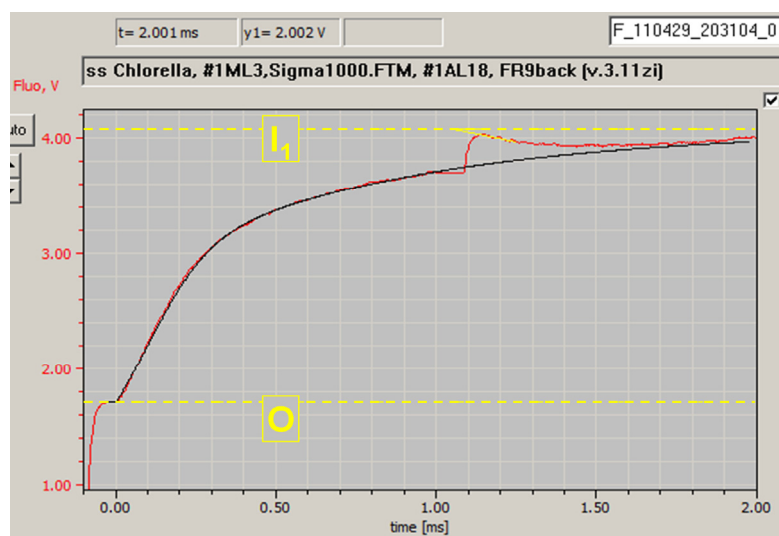|	
J	Sigmoidicity parameter, which is closely related to Joliot's connectivity parameter, p
Tau	Time constant of light-driven (by AL or MT) charge separation
Tau(reox)	Time constant of Q_A^- reoxidation.

Figure 8. Initial increase of fluorescence yield (O-I_1 rise) in a dilute suspension of *Chlorella* (300 µg Chl/L) induced by 440 nm AL at intensity setting 18 (2131 µmol quanta/(m²·s)) in presence of far-red background light. Dashed yellow lines indicate Fo-level (O), assessed during a 50 µs period preceding onset of AL at time zero, and the I_1-level that is determined with the help of a saturating single turnover pulse (ST) triggered 1 ms after onset of AL. The slope of the relaxation kinetics is extrapolated to the end of the 50 µs ST. The black line represents the O-I_1 fit curve based on a PS II model which incorporates energy transfer between PS II units and reoxidation of the primary PS II acceptor Q_A (see text).

Directly measured parameters are the Fo and I_1-levels, which define the total range of ΔF, that can be induced by a saturating ST in the presence of an oxidized PQ-pool

While determination of Tau and, hence, of k(II) = 1/Tau, does not require knowledge of PAR, the PAR has to be specified for calculation of Sigma(II)$_\lambda$, the wavelength-dependent functional cross-section of PS II. Therefore, precise measurement of PAR under the optical conditions encountered by the sample is essential for accurate Sigma(II)$_\lambda$ determination, which again is a prerequisite for transformation of PAR into PAR(II) and calculation of absolute PS II turnover rates, ETR(II) (see below). For this purpose the PamWin software provides the special <Measure PAR Lists> routine for automated determination of the PAR-values of AL, MT and MF-max for all colors offered by the Multi-Color-PAM.

For the O-I_1 rise driven by 2131 µmol quanta/(m² · s) of 440 nm AL (displayed in Fig. 8), the following values were estimated by the O-I_1 fit routine :

$$\text{Tau} = 0.173 \text{ ms}$$

$$\text{k(II)} = 1/\text{Tau} = 5.78 \cdot 10^3 \text{ s}^{-1}$$

$$\text{Tau(reox)} = 0.340 \text{ ms}$$

$$J = 2.01 \text{ (corresponding to p = 0.67)}$$

$$\text{Sigma(II)}_{440} = 4.51 \text{ nm}^2$$

With the help of these experimental data an example of step-by-step calculation of Sigma(II) may be illustrated, which in practice is carried out within fractions of a second by the PamWin software:

1) 1 µmol quanta/(m² · s) corresponds to $10^{-6} \cdot 6.022 \cdot 10^{23}$ quanta/(m² · s) (where $6.022 \cdot 10^{23}$ mol^{-1} is Avogadro's constant), which is equivalent to $6.022 \cdot 10^{-4}$ quanta · nm^{-2} · ms^{-1} (as 1 m² corresponds to 10^{18} nm²).

2) 2131 µmol quanta/(m² · s) correspond to 1.283 quanta nm^{-2} · ms^{-1}.

3) During the period of Tau = 0.173 ms (i.e. the experimentally determined PS II turnover time under the given conditions) $1.283 \cdot 0.173 = 0.222$ quanta nm^{-2} are absorbed.

4) Hence, $1/0.222 = 4.505$ nm² correspond **to the functional PS II cross section in *Chlorella* for a 440 nm quantum**, which is called **Sigma(II)$_{440}$**. This cross-section may be visualized as the effective area of a PS II unit, exposed to a beam of photons, with the size of this area varying not only with pigment composition, but also with the color of the incident light.

The above derived value of Sigma(II)$_{440}$ specifically describes the PS II efficiency of 440 nm AL for a dilute suspension of *Chlorella* under the standard condition of a non-energized sample with far-red background light. With a different AL color or another type of sample a different Sigma(II) will apply, which can be readily deter-

mined by the MULTI-COLOR-PAM via another measurement of the O-I_1 fluorescence rise followed by fitting of the time constant Tau and calculation of Sigma(II)$_\lambda$.

Calculation of Sigma(II)$_\lambda$ by the MULTI-COLOR-PAM software is based on the following general equation:

$$\textbf{Sigma(II)}_\lambda = \frac{\textbf{k(II)}}{\textbf{L} \cdot \textbf{PAR}} = \frac{1}{\textbf{Tau} \cdot \textbf{L} \cdot \textbf{PAR}} \quad\quad (3)$$

where L is Avogadro's constant, Tau is the time constant of PS II turnover during the O-I_1 rise, PAR is the quantum flux density of the light driving the O-I_1 rise and Sigma(II)$_\lambda$ is the wavelength and sample-dependent functional absorption cross-section of PS II.

In practice, the value of Sigma(II)$_\lambda$ is calculated by substituting the general terms in the equation by the experimentally determined numbers with their corresponding units, e.g. in the case of the measurement of Fig. 8, with Tau = 0.173 ms and PAR = 2131 µmol/(m² · s):

$$\text{Sigma(II)}_{440} = \cfrac{1}{0.173 \cdot 10^{-3}\,\text{s} \cdot \cfrac{6.022 \cdot 10^{23}}{\text{mol}} \cdot \cfrac{2131 \cdot 10^{-6}\,\text{mol}}{\text{m}^2 \cdot \text{s}}}$$

$$= \frac{\text{m}^2}{0.173 \cdot 6.022 \cdot 2131 \cdot 10^{14}}$$

$$= \frac{10^4\,\text{nm}^2}{0.173 \cdot 6.022 \cdot 2131}$$

$$= 4.51\,\text{nm}^2 \text{ (area per PS II for absorption of}$$
$$440 \text{ nm quanta in Chlorella)}$$

This definition of Sigma(II)$_\lambda$ relates to the functional cross-section of PS II for the specific conditions under which the O-I_1 rise measurement was carried out. Sigma(II)$_\lambda$ specifically applies for the reference state of a dark-adapted sample with open PS II reaction centers and oxidized PQ pool. It is *not* identical to the functional PS II cross-section, $\sigma_{\text{PS II}}$, defined in a less specific way (e.g. by Kolber et al. 1998) and, hence, can be modulated by changes in the PQ-redox state and various types of non-photochemical quenching.

Fig. 9 shows Sigma(II) values as a function of AL-color for a dilute suspension of *Chlorella*. O-I_1 rise kinetics similar to the one shown in Fig. 8 were measured with the help of a pre-programmed script-file (Sigma1000Chlor_10.prg) for the five different AL-colors with 10 s time intervals between consecutive measurements. Continuous far-red background light was applied in order to keep the PQ-pool oxidized. Sigma(II)$_\lambda$ was determined by fitting the O-I_1 rise curve as described for the curve in Fig. 8.

By comparing the Sigma(II) and Fo/PAR spectra for *Chlorella* in Fig. 9 and Fig. 2, respectively, it is apparent that Sigma(II) and Fo/PAR carry very similar information on PS II absorption of a sample. An important difference, however, is that Sigma(II) gives absolute information on the functional cross-section of PS II, which is independent of Chl content, whereas Fo/PAR is proportional to

both Chl content and functional cross-section of PS II. Furthermore Fo/PAR depends on ML-intensity and gain parameters, which have no influence on Sigma(II), as measured with the MULTI-COLOR-PAM.

3.3   Definition of PAR(II) and ETR(II)

The wavelength-dependent PS II-effective quantum flux *rate* is directly reflected in the **k(II)** determined by fitting the O-I_1 rise kinetics measured at high PAR. There is direct correspondence between the PS II turnover rate, k(II), in units of electrons/(PS II · s) and the quantum absorption rate at PS II reaction centers in units of quanta/(PS II · s). We propose the name PAR(II) for the latter, with the general definition derived from equation 3 above:

$$\textbf{PAR(II)} = \textbf{k(II)} = \textbf{Sigma(II)}_\lambda \cdot \textbf{L} \cdot \textbf{PAR} \qquad (4)$$

where k(II) is the rate constant of PS II turnover, Sigma(II)$_\lambda$ is the functional cross-section of PS II, L is Avogadro's constant, PAR is the quantum flux density of illumination and PAR(II) is the rate of quantum absorption in PS II. PAR(II) is expressed in **units of quanta/(PS II · s).**

In practice, PAR(II) is calculated by substituting the general terms in this equation by the experimentally determined values with their corresponding units (see example below). Most importantly, once Sigma(II) has been determined for one particular color and sample (via measurement of the O-I_1 rise kinetics at a defined high light intensity), k(II) and PAR(II) can be derived for any other PAR, without any further measurements of fast kinetics.

An essential difference between PAR(II) and PAR is that

Figure 9. Functional cross-section of PS II, Sigma(II) as a function of AL-color in a dilute suspension of *Chlorella* (300 µg Chl/L) derived from automated measurement of 5 consecutive O-I_1 rise curves (Script-file Sigma1000Chlor_10.prg) in the presence of far-red background light at intensity level 1 (FR 1).

the former relates to the quantum absorption *rate* of PS II, which is independent of Chl content, whereas the latter represents a quantum *flux density,* from which a PS II quantum absorption rate can be calculated only, if the PS II content is known.

Consequently, based on PAR(II), also a wavelength- and sample-dependent ETR(II) can be defined:
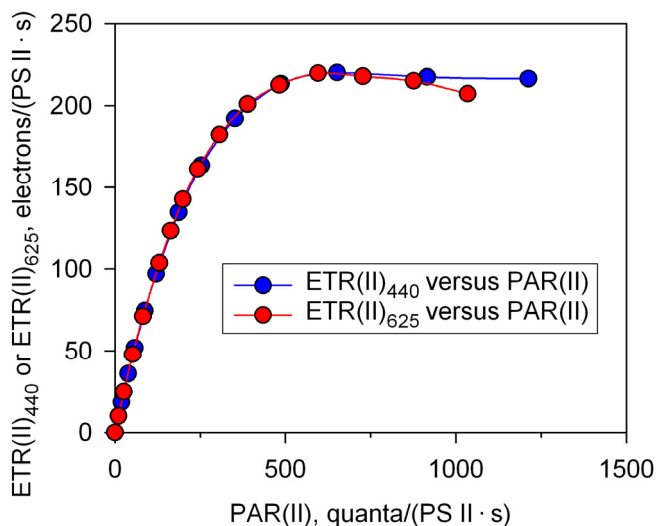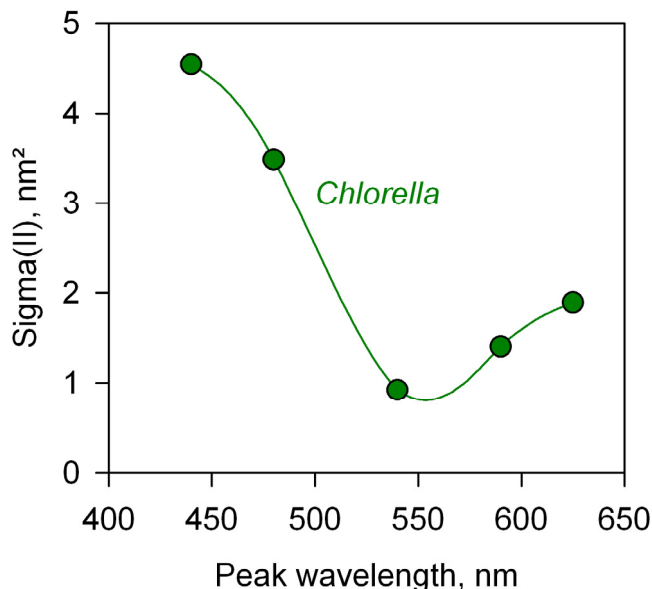
Figure 10. Comparison of ETR(II) light curves measured with dilute *Chlorella* suspension (300 µg Chl/L) using 440 nm and 625 nm actinic light after transformation of the original PAR scale into a PAR(II) scale (see text). Sigma(II) values of 4.51 and 1.71 nm² were applied for 440 and 625 nm, respectively. In the calculation of ETR(II)$_{440}$ and ETR(II)$_{625}$ Fv/Fm-values of 0.68 and 0.66 were used, respectively. For comparison of the corresponding LC without PAR transformation, see Fig. 11.
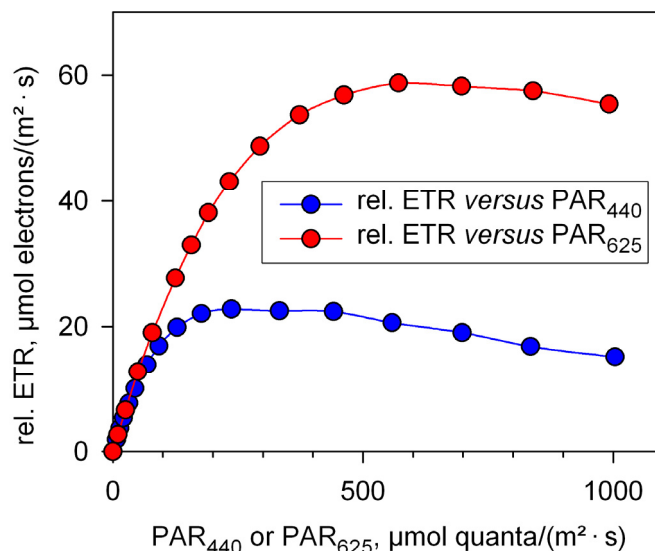
Figure 11. Comparison of rel. ETR light curves measured with 440 and 625 nm AL using the original PAR scale. A screenshot of the 440 nm curve has already been shown in Fig. 6.

$$\mathbf{ETR(II) = PAR(II) \cdot \frac{Y(II)}{Y(II)_{max}}} \qquad (5)$$

where PAR(II) is the rate of quantum absorption at PS II, Y(II) the effective PS II quantum yield derived from the fluorescence ratio parameter (Fm'-F)/Fm', $Y(II)_{max}$ the PS II quantum yield in the quasi-dark reference state under which $Sigma(II)_\lambda$ was determined and ETR(II) the rate of electron transport expressed in **units of electrons/(PS II · s)**.

At very low light intensity, Y(II) approaches $Y(II)_{max}$, so that $Y(II)/Y(II)_{max} = 1$ and ETR(II) = PAR(II). This means that there is no loss of PS II efficiency with respect to the reference quasi-dark state (all centers open, non-energized, weak far-red background illumination) under which $Sigma(II)_\lambda$ was measured. $Y(II)_{max}$ corresponds to the PS II quantum yield of a sample in the same state as given for measurement of k(II) (see e.g. Fig. 5), which equals Fv/Fm. In measurements with algae and cyanobacteria, which may display a relatively high level of PQ-reduction in the dark, it is advisable to measure Fv/Fm in the presence of far-red background light, which oxidizes the PQ-pool and induces the high PS II-efficiency "state I". Far-red background light is also routinely used for assessment of k(II) and $Sigma(II)_\lambda$ via the $O\text{-}I_1$ rise kinetics.

When compared with the common definition of rel. ETR in equation (2), it is apparent that the ETR-factor is contained in PAR(II) and that ETR(II) has the dimension of a turnover rate per PS II, whereas rel. ETR commonly has been treated as an electron flux density, i.e. a rate per area, which without information on PS II per area must be considered fictive. In contrast, ETR(II) realistically describes the mean absolute rate of charge separation per PS II in all PS II contained in the 1 mL investigated sample. In practical work with the MULTI-COLOR-PAM, the color and intensity of the applied actinic light as well as the type of investigated samples may be frequently changed. While changes in PAR are accounted for by the PAR-lists, a new $Sigma(II)_\lambda$ determination is required when the type of sample and/or the color are changed.

When the appropriate wavelength- and sample-dependent $Sigma(II)_\lambda$ value is known, the user software supports the transformation of the PAR-lists into corresponding PAR(II)-lists. A practical example of transformation of a PAR-scale into a PAR(II) scale is given in Fig. 10, where the blue curve shows the same ETR Light Curve data as presented in Fig. 5, but presented with a PAR(II) light intensity scale. Transformation of PAR-values into PAR(II) values is based on equation 4. The following step-by-step example of calculation applies for PAR = 237 µmol quanta/(m² · s) of 440 nm light using the same *Chlorella* suspension, with which the data of Figs. 5, 6, 8, 10, and 11 were collected:

$$PAR(II)_{440} = Sigma(II)_{400} \cdot L \cdot PAR$$

$$= 4.51\,nm^2 \cdot \frac{6.022 \cdot 10^{23}}{mol} \cdot \frac{237 \cdot 10^{-6}\,mol}{m^2 \cdot s}$$

$$= 4.51 \cdot 10^{-18}\,m^2 \cdot \frac{6.022 \cdot 10^{23}}{mol} \cdot \frac{237 \cdot 10^{-6}\,mol}{m^2 \cdot s}$$

$$= 644\,s^{-1}(\text{quanta absorbed per PS II and s})$$

This calculation is automatically carried out by the PamWin software for all PAR-values at which quantum yields where measured in conjunction with a Light Curve, when the PAR-scale is transformed into a PAR(II) scale.

The corresponding $ETR(II)_{440}$ value is calculated according to general equation 5, by entering the values of PAR(II) (with the corresponding unit) and Y(II) = 0.23 for PAR = 237 µmol quanta/(m² · s) as well as $Y(II)_{max} = 0.68$ for the dark-adapted sample in presence of far-red background light (i.e. condition under which $Sigma(II)_{440}$ was measured):

$$ETR(II)_{440} = PAR(II)_{440} \cdot \frac{Y(II)}{Y(II)_{max}}$$

$$= 644\,s^{-1} \cdot \frac{0.23}{0.68}$$

$$= 218\,s^{-1}\,(\text{electrons transported}$$
$$\text{per PS II and s})$$

After transformation of PAR into PAR(II), the ETR(II) light curves (LC) measured with different AL colors can be directly compared. The red curve in Fig. 10 shows the corresponding $ETR(II)_{625}$ LC measured with the same dilute Chlorella sample, the parameters of which obtained *before* PAR-transformation were already shown in Figure 7. For comparison, Fig. 11 shows the original LC curves of rel. ETR with 440 and 625 nm AL *before* transformation of PAR into PAR(II).

Comparison of the data in Figs. 10 and 11 reveals the distinct advantage of transformation of PAR into PAR(II). Whereas before transformation the maximal rel. values differed by a factor of 2.58, after transformation the $ETR(II)_{440}$ and $ETR(II)_{625}$ are practically equal. This may be considered strong support for the validity of $Sigma(II)_\lambda$ determination via $O\text{-}I_1$ measurements with the MULTI-COLOR-PAM and its analysis by the $O\text{-}I_1$ Fit approach.

When information on PS II concentration is available, this may serve to derive an estimate of absolute O_2 evolution rate with the common unit of µmol O_2/(mg Chl · h) from ETR(II). As will be shown below, a very simple general equation can be applied for this calculation. For understanding the background, however, reading the following points may be useful, with step-by-step calculations specifically for the experiment of Fig. 10 with PAR = 237 µmol quanta/(m² · s) of 440 nm light, for which calculation of PAR(II) and ETR(II) already was outlined above:

1) In the MULTI-COLOR-PAM cuvette an area of 100 mm^2 is illuminated. As measurements are carried out with highly dilute samples, it may be assumed that the incident PAR (measured either with the planar sensor MQS-B at the exit of the 10 x 10 mm *Perspex* light guide rod or with the spherical sensor US-SQS/B within the 10 x 10 mm cuvette) is effective throughout the whole sample. Hence, the number of PS II units within 1 mL of the investigated suspension is decisive for the absolute rate.

2) The overall Chl content of the *Chlorella* suspension equals 300 µg Chl/L, which corresponds to $3 \cdot 10^{-7}$ g Chl/mL.

3) This amounts to $3.333 \cdot 10^{-10}$ mol Chl/mL, assuming a molecular weight of 900 g/mol for Chl.

4) As one mol contains $6.022 \cdot 10^{23}$ molecules, this corresponds to $2.01 \cdot 10^{14}$ molecules of Chl/mL.

5) Assuming a photosynthetic unit (PSU) size of 1000 Chl molecules per electron transport chain (including one PS II each), it follows that about $2.01 \cdot 10^{11}$ PS II are contained in the illuminated 1 mL suspension. Based on this information, a volume related electron transport rate can be calculated from

ETR(II)$_{440}$=218 electrons/(PS II · s):

6) Electrons transported by all PS II contained in 1 mL suspension:

$$re^- = 218 \cdot 2.01 \cdot 10^{11} = 438 \cdot 10^{11} \frac{electrons}{mL \cdot s}$$

and, as 4 electrons are transported by PS II for evolution of one molecule O_2 and 1 h = 3600 s, the corresponding volume related O_2 evolution rate amounts to

$$rO_2 = 438 \cdot 10^{11} \cdot \frac{3600}{4} = 3.94 \cdot 10^{16} \cdot \frac{molecules\, O_2}{mL \cdot h}$$

$$= \frac{3.94 \cdot 10^{16}}{6.022 \cdot 10^{23}} = 0.654 \cdot 10^{-7} \frac{mol\, O_2}{mL \cdot h}$$

which is the absolute rate at which the O_2 concentration in the sample increases with time, as it can be also directly measured with an O_2-electrode.

7) In physiological work, photosynthetic electron transport rate often is expressed in µmol O_2/(mg Chl · h), i.e. Chl mass related rO_2. For transformation into these units it has to be considered that 1 mL of 300 µg Chl/L suspension contains $3 \cdot 10^{-4}$ mg Chl

$$rO_2 = \frac{0.654 \cdot 10^{-7}}{3 \cdot 10^{-4}} \frac{mol\, O_2}{mL \cdot h} = 218 \frac{\mu mol\, O_2}{mg\, Chl \cdot h}$$

It may be noted that the numerical value of the rate expressed in µmol O_2/(mg Chl · h) is identical to that expressed in electrons/(PS II · s). This simple relationship, however, is valid only with the specific assumptions made above, i.e. a functional photosynthetic unit (PSU)

size of 1000 Chl/PSU and a molecular weight of Chl of 900 g/mol.

The absolute rate of O_2-evolution in units of mmol O_2/(mg Chl · s) can be derived from ETR(II) by the following general equation:

$$rO_2 = \frac{ETR(II)}{PSU \cdot ne(O_2) \cdot M(Chl)} \tag{6}$$

where M(Chl) is the molecular weight of Chl and ne(O_2) the number of electrons required for evolution of 1 molecule of O_2 (normally assumed to be 4). The absolute rate in the common units of µmol O_2/(mg Chl · h) is obtained by multiplication with 3600 · 1000. As one can see, the identical numerical values for ETR(II) in electrons/(PS II · s) and rO_2 in µmol O_2/(mg Chl · h) is owed to the coincidence that the molecular weight of Chl times ne(O_2)=4 equals the number of seconds in one hour.

3.4 Leaf measurements

For measurements with leaves a special leaf holder is available, measuring fluorescence from the leaf surface. As high chlorophyll content is unavoidable in the case of leaves, pronounced light intensity gradients are the rule, even with green light, resulting in heterogeneous photosynthetic responses in different cell layers at varying depths from the illuminated surface (see e.g. Vogelmann 1993; Schreiber et al. 1996). While it is generally impossible to measure the *overall* photosynthetic response of a leaf via chlorophyll fluorescence, the MULTI-COLOR-PAM allows for relatively homogenous responses from the top cell layers at upper and lower leaf surfaces. For this purpose, two aspects are essential:

a) Use of 440 nm pulse-modulated measuring light (ML), which is almost completely absorbed within the top cell layer.

b) Use of a short-pass filter (< 710 nm) in front of the detector, so that selectively short-wavelength fluorescence is measured, which almost completely originates from the top cell layer, as most of the short-wavelength fluorescence that is excited within deeper layers (despite of the use of 440 nm ML) will be reabsorbed by the chloroplasts in the upper cell layers.

Figs. 12 and 13 show fluorescence responses (F<710 nm) measured from the upper (adaxial) and lower (abaxial) surfaces of the same ivy leaf using 440 nm ML. In the experiment of Fig. 12 the dark-adapted leaf was illuminated with continuous 440 nm AL starting at time 0, resulting in typical dark-light induction curves (Kautsky effect).

The dark-light induction kinetics of upper and lower leaf sides differ considerably, although the same intensity of AL is applied (see also Schreiber et al. 1977). While a detailed discussion of the differences would be out of the scope of the present communication, it may be noted that the response of the lower leaf side is more pronounced,

just as if the applied PAR were higher. In principle, this could be either due to a larger functional cross-section of PS II, Sigma(II)$_{440}$, or to a smaller acceptor pool size in the shade-adapted lower leaf side. Fig. 13 shows O-I1 rise curves measured from upper (left) and lower (right) sides of the same ivy leaf. As already is obvious by visual comparison, the initial slope is significantly higher at the lower than at the upper leaf side. Upon fitting of the two curves 32% larger values of k(II) and Sigma(II)$_{440}$ are suggested for the lower vs. the upper leaf surface.
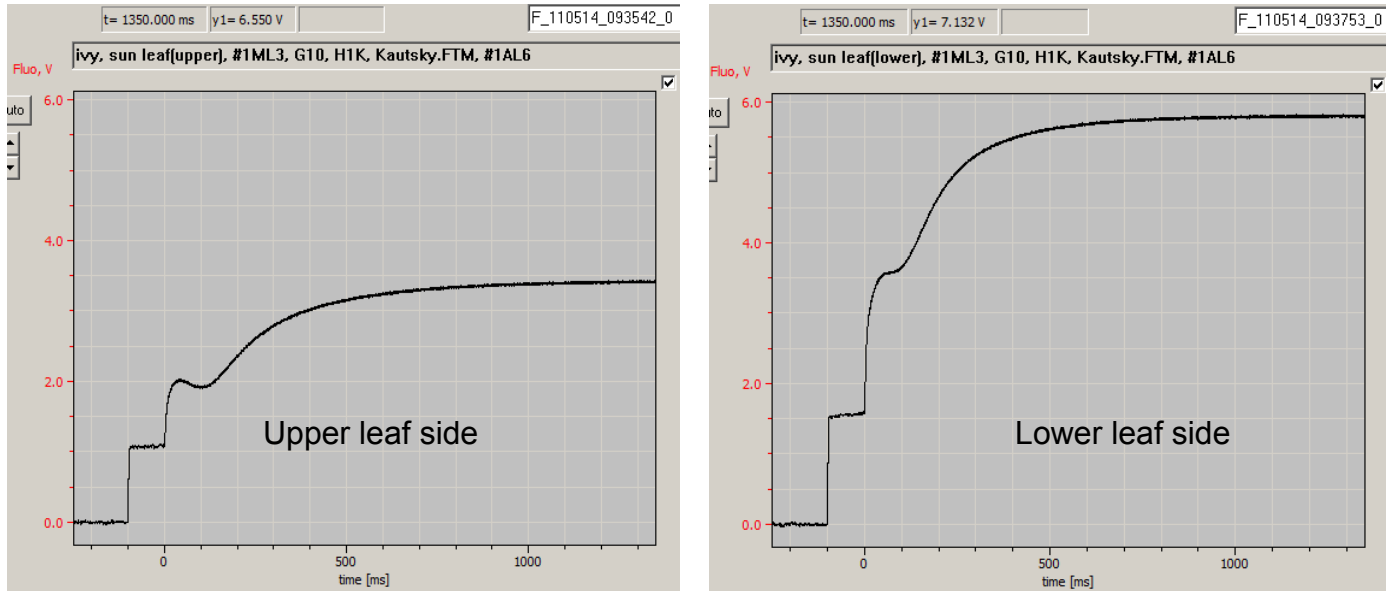

Figure 12. Dark-light induction curves (Kautsky effect) of ivy leaf measured from upper (left curve) and lower (right curve) sides of the same leaf. 440 nm ML switched on 100 ms before onset of actinic illumination (118 µmol quanta m^{-2} s^{-1} 440 nm) at time 0. Fluorescence detection at wavelengths < 710nm.
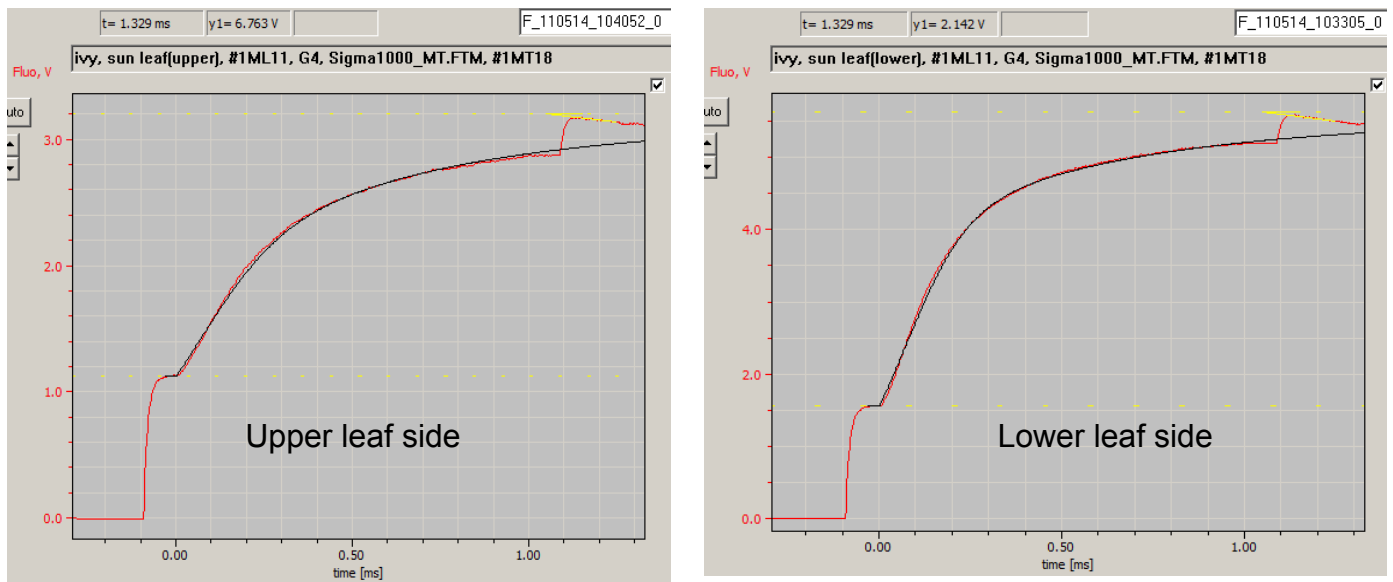

Figure 13. O-I1 rise curves induced by strong actinic light (440 nm multiple turnover pulse, MT) at upper (left curve) and lower (right curve) sides of the same ivy leaf. The two curves are normalized at the I$_1$-level. Dashed yellow lines indicate the Fo-level (O) assessed during a 50 µs period preceding onset of at time zero and the I$_1$-level that is determined with the help of a saturating multi-color single-turnover pulse (ST) triggered 1ms after onset of MT. The slope of the relaxation kinetics is extrapolated to the end of the 50 µs ST. The black line represents the O-I$_1$ fit curve based on a PS II model which incorporates energy transfer between PS II units and reoxidation of the primary PS II acceptor Q$_A$ (see text to Fig. 8).

4 Single turnover pulses, ST

4.1 General features

The same multi-color LED array that generates AL, is also employed for generating single turnover light pulses, ST. The user may choose between ST with one of 6 different colors (440, 480, 540, 590, 625 nm and white) and "multi-color ST", with all of these 6 colors being applied simultaneously. A multi-color ST at 50 µs width normally is saturating, which is not necessarily true for single color ST. For Fast Kinetics recordings, ST can be programmed with 2.5 to 50 µs width.

The duration of single turnover pulses is so short that not more than one charge separation per PS II reaction center is possible, as the reoxidation of the primary PS II acceptor Q_A by the secondary acceptor Q_B is characterized by time constants in the order of 200-600 µs. ST-induced Q_A reduction and the ensuing reoxidation kinetics can be readily measured in the fast kinetics mode of the MULTI-COLOR-PAM (Fig. 14). In many applications it is essential that the applied ST pulses are saturating, which means that all PS II reaction centers turn over once and, hence, a maximal increase of fluorescence yield is obtained.

4.2 ST-efficiency and exponential saturation characteristics

The ST-efficiency, i.e. the extent of ST-induced fluorescence increase depends on a number of parameters, namely:

- Choice of ST color or Multi-Color

- Selected ST width

- Chlorophyll content of the sample

- PS II antenna composition of the sample

- Filter in front of the photodetector (particularly with dense samples, like leaves)

- Choice of ML color (particularly with dense samples, like leaves).

The MULTI-COLOR-PAM displays exceptionally high sensitivity, so that rather low chlorophyll content is feasible, which favors high ST-efficiency (practically no shading). Measurements at low Chl content are also advantageous, because light-intensity gradients are avoided. This is particularly important, for evaluation of the light-saturation characteristics and assessment of potential heterogeneities in PS II antenna size (Melis 1991, Lavergne and Briantais 1996).

The data presented in Figs.14 and 15 were obtained with a dilute suspension of *Chlorella vulgaris* at a Chl *a* content of 400 µg/L (green color just visible). Fast relaxation kinetics in response to multi-color ST pulses of various widths (5, 10, 20 and 50 µs) are shown in Fig. 14. The

sample was continuously illuminated with far-red background light in order to establish defined conditions in terms of PS II acceptor side oxidation and pigment state 1.

Analogous data were collected for additional ST-widths (i.e. 2.5, 7.5, 12.5, 15, 30 and 40 µs, kinetics not shown) and a corresponding set of data was collected using 440 nm ST pulses (kinetics not shown). These measurements were carried out with the help of a preprogrammed script-file (STwidth_relax.prg), which automatically opens the corresponding Fast Trigger files for measuring the ST-induced fluorescence increase followed by the relaxation kinetics. Under the given conditions with multi-color ST pulses close to saturation is already reached with 20 µs width, whereas 50 µs width is required in the case of 440 nm ST pulses.

The saturation curves of the ST-induced fluorescence increase (ΔF) as a function of ST-width are presented in Fig. 15 for both multi-color and 440 nm ST pulses. As the pulses display steep on/off slopes, ST width is proportional to ST pulse energy and, hence, the plot of the ST-induced ΔF vs. ST width corresponds to classical flash energy saturation curves (Falkowski et al. 1986, Mauzerall and Greenbaum 1989). From the data in Fig. 15 it can be estimated that with a dilute *Chlorella* suspension the multi-color ST are about 2.3 times more effective in terms of PS II turnover than the 440 nm ST. In the given example, even a single-color (440 nm) 50 µs ST is saturating. While the 440 nm LED chips amount to only about 14% of the overall number of actinic chips, the 440 nm light is particularly well absorbed in *Chlorella*.

4.3 ST-pulse intensity and functional PS II cross-section Sigma(II)$_\lambda$

The light intensity corresponding to a 440 nm ST pulse can be deduced by comparison with the response of the same sample to a 440 nm AL or MT pulse (see section below), the intensity of which can be directly measured. The ΔF induced by a 50µs 440 nm AL pulse of 3613 µmol quanta/(m² · s) matches the ΔF induced by a 3.6 µs 440 nm ST. Ignoring Q_A^- reoxidation and assuming that the initial rise of ΔF vs. ST-width is linear, in first approximation it may be assumed that the quantum flux density in the 440 nm ST pulse is 50/3.6=13.88 times higher than in the 440 nm AL pulse. Then 440 nm ST-pulse intensity amounts to $13.88 \cdot 3613 = 50180$ µmol quanta/(m² · s) and a 50µs ST pulse contains $1.51 \cdot 10^{18}$ quanta/m² (Avogadro's constant $L = 6.022 \cdot 10^{23}$ mol^{-1}). Based on this information and on the 440 nm ST saturation curve in Fig. 15, the MULTI-COLOR-PAM provides an alternative method for estimation of the wavelength-dependent functional PS II absorption cross-section, Sigma(II)$_\lambda$ (for determination by analysis of O-I$_1$ rise ki-
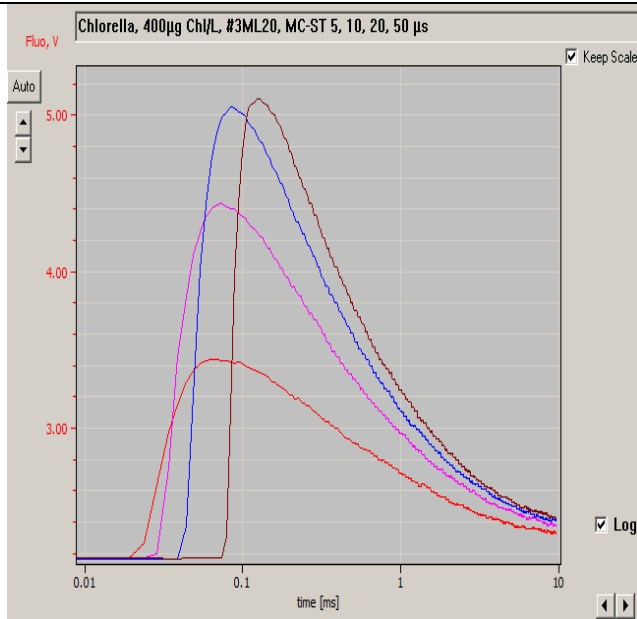
Figure 14. Multi-color ST-induced fluorescence increase in dilute *Chlorella*-suspension (400 µg Chl/L) at ST-widths of 5, 10, 20 and 50 µs. Fluorescence excitation with #3ML (540 nm). Continuous far-red background illumination (FR 9). Relaxation curves displayed with Log time scale.
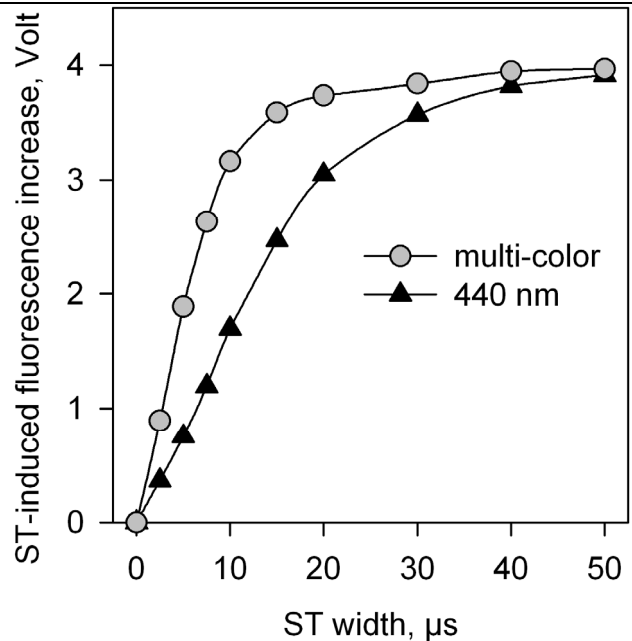

Figure 15. ST-induced fluorescence increase in dilute suspension of *Chlorella vulgaris* as function of the width of ST pulses applied either with the single color #1 (440 nm) or with the combination of all colors (Multi-Color). Examples of Multi-Color ST-induced relaxation kinetics are shown in Fig.14.

netics, see section 3.2). An example of application of this method is described here in some detail, in order to show the basic equivalence between the classical "single-turnover flash saturation" and the "O-I$_1$ fit" approaches.

The light-induced closure of PS II reaction centers by ST-pulses with increasing pulse widths in first approximation can be described assuming simple exponential saturation characteristics according to:

$$\frac{\Delta F}{\Delta F_{sat}} = 1 - e^{-Sigma(II)_{440} \cdot L \cdot PAR \cdot t} \qquad (7)$$

where ΔF is the increase of fluorescence yield with the ST-width corresponding to time t (s), ΔF_{sat} the maximal increase of fluorescence yield with a saturating ST, Sigma(II)$_{440}$ the PS II absorption cross-section for 440 nm quanta (m²), L the Avogadro constant (mol^{-1}) and PAR the quantum flux density in mol/(m² · s) during the ST.

An average of 63% of PS II centers are closed when Sigma(II)$_{440}$ · PAR · L · t = 1 and, hence, $\Delta F = \Delta F_{sat}$ (1-1/e), i.e. when ΔF is 63% of the saturated ΔF. From the 440 nm ST saturation curve in Fig. 15 it can be estimated that this response is obtained with a 15.17 µs ST, which corresponds to $0.474 \cdot 10^{18}$ quanta/m². Hence, for one 440 nm quantum the effective cross-section area is 2.18 nm², which is Sigma(II)$_{440}$. This value of Sigma(II)$_{440}$ is significantly lower than the 4.51 nm² determined for *Chlorella* via analysis of the O-I$_1$ rise (see section 3.2). It should be noted that in the ST-based approximation of Sigma(II)$_\lambda$, linearity between ΔF and Q$_A^-$ is assumed, whereas in reality the relationship is non-

linear due to energy transfer between PS II units (Joliot and Joliot 1967). Furthermore, reoxidation of Q$_A^-$ during the ST and the ensuing time period before measurement of fluorescence yield is not taken into account, which results in underestimation of Sigma(II). Last but not least also an intrinsic inefficiency of charge separation at very high light intensities (Rappaport et al. 2007) could be responsible for a lower value of Sigma(II) when measured by the ST-saturation approach as compared to the O-I$_1$ fit approach.
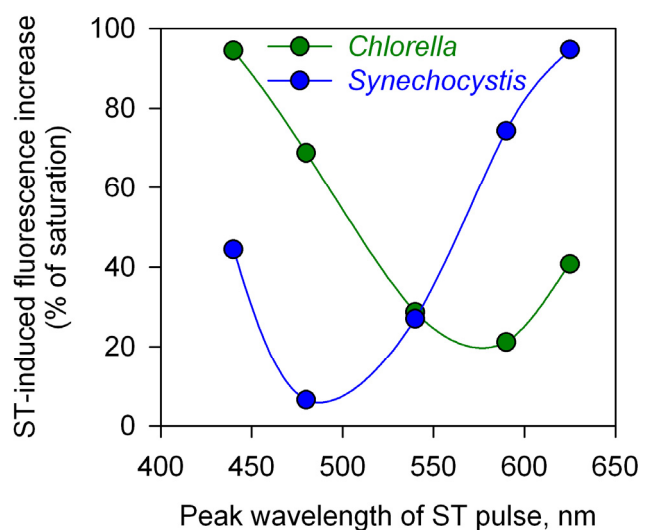

Figure 16. Fluorescence increases induced by 50 µs ST pulses of various colors in dilute suspensions of *Chlorella* and *Synechocystis* in relation to the saturating effect of a 50 µs multi-color ST (100%). Fluorescence excitation with 540nm. Continuous far-red background illumination (FR 9).

Hence, although the MULTI-COLOR-PAM provides the means to estimate Sigma(II) via classical flash saturation curves, measurements of the O-I$_1$ rise kinetics and determination of Sigma(II) with the help of the O-I$_1$ fitting routine provided by the PamWin software are not only more rapid and convenient, but also more reliable for 3 major reasons:

- relatively moderate actinic intensity is used, thus minimizing inefficiency caused by extremely high quantum flux densities;
- the connectivity/sigmoidicity parameter J is fitted, so that non-linearity between ΔF and Q$_A$$^-$ can be accounted for;
- the applied PS II model takes account of Q$_A$$^-$ oxidation by Q$_B$.

4.4 Relative ST pulse effects of the various colors in Chlorella and Synechocystis

The fluorescence increases (ΔF) induced by variously colored ST pulses in differently pigmented organisms like *Chlorella* and *Synechocystis* depend on the ST pulse energy (quanta·m²) and the wavelength-dependent functional cross-section of PS II, Sigma(II)$_λ$, of the investigated sample. While for technical reasons saturation cannot be reached with all single colors, this is always possible using a Multi-Color ST. Hence, the effect of variously colored ST pulses can be quantified relative to the saturated effect induced by a Multi-Color ST (see Fig. 16).

It may be noted that there is some similarity between the spectra of ST-induced ΔF in Fig. 16, of Fo/PAR in Fig. 2 and of Sigma(II) in Fig. 9. This is true, although the ST-intensities of the various colors differ from each other. In first approximation, the relative differences may be estimated from the PAR-values at maximal AL-intensity settings presented in Table 3. In this way, spectra of ΔF(ST)/PAR can be derived (not shown) that provide similar information as Sigma(II) spectra. The practical value of such spectra decisively depends on the accuracy, with which the ST intensities of the various colors can be measured.

5 Multiple turnover pulses, MT and saturation pulses, SP

5.1 General features

The same multi-color LED array that generates AL and ST, is also employed for generating "Multiple Turnover" light pulses, MT and Saturation Pulses, SP. There is no principal difference between AL and MT/SP, except for three features:

a) Maximal MT/SP intensities can be more than twice higher than the corresponding maximal AL intensities.

b) Maximal MT/SP width is limited to 800 ms, whereas AL can be applied for an unlimited time.

c) The increase of MT/SP intensity with increasing settings is close to linear, whereas it is exponential in the case of AL.

The user may choose between one of 6 different colors (440, 480, 540, 590, 625 nm and white), which at the same time apply for AL, MT/SP and ST.

While MT pulses and SP do not differ physically, they serve different functions in PAM fluorimetry. MT pulses are mostly used with Fast Kinetics recordings. They can be programmed in Fast Trigger files. For maximal kinetic resolution normally switching to MF-max (100 or 200 kHz) is triggered. On the other hand, SP are used for Saturation Pulse quenching analysis, e.g. in conjunction with Slow Kinetics and Light Curve recordings. With every SP automatically Y(II) and other fluorescence based parameters are calculated, which is not the case with MT. During an SP the frequency of pulse-modulated ML is automatically switched to 10 kHz.

Major differences between MT and ST are:

a) MT can be applied at largely different intensities, in analogy to AL. In contrast, ST are always applied at maximal intensity, with their effect being controlled by the ST-width.

b) Maximal MT-width is 800 ms, whereas ST-width is limited to a maximal value of 50μs. The minimal value is 2.5 μs.

c) With ST in contrast to MT all colors can be applied simultaneously.

For each color the user may choose between 20 MT intensity settings, corresponding to defined LED currents and PAR values at the exit of the *Perspex* light guide of the emitter unit. For standard applications default current/PAR lists (default_MC.par and default_leaf.par) with close to linearly increasing intensity steps are provided.

The default lists can be readily modified by the user and saved in new par-files. LED current values can be programmed in 255 steps.

The PAR values defined in the default lists were measured with the help of the automated <Measure PAR Lists> routine using the US-SQS/B and MQS/B sensors (Walz) for suspension cuvette and leaf holder, respectively. These sensors can resolve the kinetics of short light pulses and determine the PAR during the first milliseconds of the pulse. This is important, as the LED-chips unavoidably heat up with high current pulses, which leads to significant drops of intensity within the 10-100 ms time range (particularly in the case of the 590 and 625 nm LEDs, which display a relatively high temperature coefficient). Accurate PAR-measurements are essential in conjunction with determination of the wavelength dependent functional cross-section of PS II,

Sigma(II)$_\lambda$ (see section 3.3). As the O-I$_1$ measurement is terminated after 1-2 ms, it is not disturbed by the heating of the LED-chips during an MT pulse.

Depending on the selected width, MT/SP in contrast to ST pulses can induce multiple turnovers at PS II reaction centers and thus cause full reduction not only of the primary acceptor Q$_A$, but also of Q$_B$ and the plastoquinone acceptor pool, PQ, which is required for assessment of maximal fluorescence yield Fm or Fm'(see Schreiber 2004). An SP serves the function of inducing full reduction of the acceptor side, for which purpose the color, intensity and width have to be appropriately selected. The SP kinetics, which are automatically saved under Fast Kinetics, indicate whether the selected parameters are appropriate. Essential criteria are:

- A plateau level is reached.

- The intensity is not much higher than required to reach maximal amplitude. In particular, the intensity should be decreased, if the signal transiently jumps to a somewhat higher value when the SP/MT is over. This phenomenon reflects donor-side dependent quenching.

- The width is not much longer than required to reach a plateau, in order to minimize the dose of potentially harmful strong light.

The time resolution of the SP kinetics is *not* high enough for kinetic analysis of the polyphasic fluorescence rise upon onset of saturating light (O-I$_1$-I$_2$-P curve) which,

however, can be routinely measured with the help of MT pulses and preprogrammed Fast Trigger files.

5.2 Polyphasic fluorescence rise, O-I$_1$-I$_2$-P

Fig. 17 shows a typical example of a polyphasic fluorescence rise measured with a dark-adapted ivy leaf using 440 nm ML and a 440 nm MT pulse of maximal intensity (MT20). Using a logarithmic time scale the three consecutive rise phases in the ranges of 100μs (O-I$_1$), 10ms (I$_1$-I$_2$) and 100 ms (I$_2$-P) can be displayed with distinct plateau regions in between, corresponding to the intermediate levels I$_1$ and I$_2$. The clear-cut separation of the various phases is due to the following features provided by the MULTI-COLOR-PAM:

- Use of a very high light intensity, which assures full reduction of the primary acceptor Q$_A$ during the photochemical O-I$_1$ phase before onset of the first thermal phase (I$_1$-I$_2$).

- Measuring fluorescence from the surface in the case of leaves or with dilute suspensions in the case of unicellular algae or cyanobacteria.

- In the case of leaves, use of 440 nm ML for almost selective excitation of the top cell layer, where irradiance is close to homogenous;

- In the case of leaves, detection of short-wavelength fluorescence (<710 nm), so that selective assessment of the top cell layer is further enhanced.
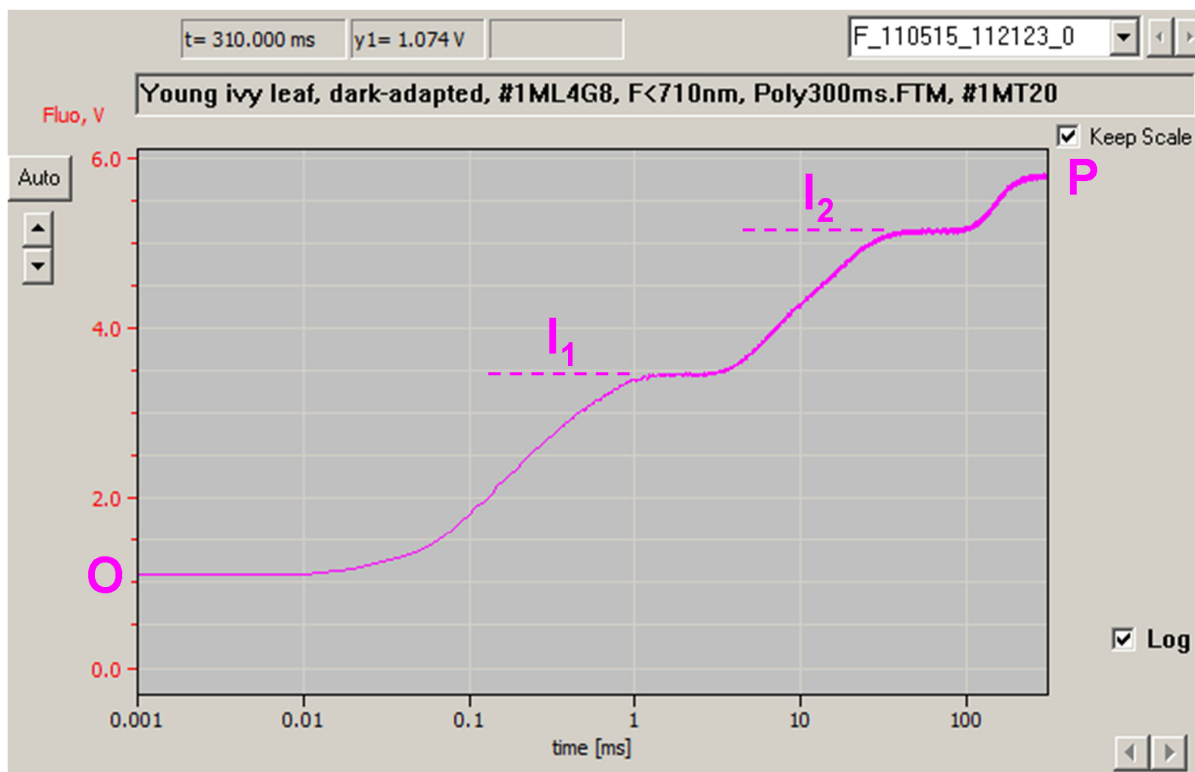

Figure 17. Polyphasic rise of fluorescence yield (F<710nm) upon onset of saturating light in dark-adapted ivy leaf (upper surface). Characteristic fluorescence levels O-I$_1$-I$_2$-P are indicated. Use of 440 nm ML and 440 nm multiple turnover pulse (MT 20). Display with logarithmic time scale.

Elimination of F>710 nm also enhances the ratio of PS II/PS I fluorescence in the measurement of PS II quantum yield, Fv/Fm and Y(II), as well as of the derived electron transport rate, ETR(II), improving their accuracy

Measurements of the O-I_1-I_2-P rise kinetics in suspensions of unicellular algae and cyanobacteria are complicated by the fact that in these organisms during dark-adaptation more or less strong electron flow from reduced stroma components to plastoquinone (PQ) takes place, so that the redox state of the PQ-pool is undefined. The latter is problematic for three reasons:

a) Reduced PQ is in equilibrium with reduced Q_B (Q_B^- and Q_B^{2-}) and Q_A^-, which may lead to overestimation of Fo and acceleration of the O-I_1 rise.

b) PQ reduction affects the quenching of fluorescence yield at the I_1-level (apparent PQ-quenching, see e.g. Schreiber 2004), thus causing uncontrolled variability of I_1.

c) PQ reduction triggers a state transition from state 1 to state 2, which may affect the functional cross-section of PS II.

In applications, where a defined state of the PS II acceptor side is essential (e.g. for determination of wavelength dependent functional cross-section of PS II, see sections 3.2 and 3.3), these problems can be avoided by far-red (FR) background light, which is provided by the MULTI-COLOR-PAM.

The multi-color Chip-on-board LED-array features a single 1x1mm far-red power-chip with peak emission at 725 nm and 30 nm half-band width. Wavelengths below 700 nm are suppressed by a long-pass filter. The user may choose between 20 FR intensity settings which are defined in the corresponding current/PAR list. In the de-

fault current/PAR list (default_MC.par) the same current values are used for FR as for 625 nm AL (see Fig. 3), i.e. currents and intensities increase exponentially with increasing settings. The default list can be readily modified by the user and the new list saved in a new par-file. LED current values can be programmed in 255 steps.

FR plays an important role in photosynthesis research and in PAM work in particular, as it is much better absorbed by PS I than by PS II. FR illumination results in oxidation of P700 and consequently of the intersystem electron transport chain, including the PQ-pool. At a given FR intensity, the relative extent of FR-induced oxidation depends on the rate at which PQ is reduced either by PS II activity, cyclic PS I activity or electron donation by stroma components in the dark.

The latter mechanism is particularly pronounced in algae and cyanobacteria, where dark reduction of the PQ-pool leads to transition from state 1 to state 2, with the latter being characterized by decreased PS II excitation. The MULTI-COLOR-PAM is ideally suited for investigations of this important regulatory mechanism. A separate PAN article on measurements of reversible state 1-state 2 transitions and assessment of the wavelength-dependent functional cross-section of PS II is in preparation.

While FR is much more effective in excitation of PS I relative to PS II, which indirectly affects fluorescence yield via the redox state of the intersystem electron transport chain, its direct effect on PS II can also be significant, particularly with respect to so-called "inactive PS II" (Lavergne and Leci 1993). The MULTI-COLOR-PAM has opened the way for a profound analysis of this type of PS II heterogeneity, which will be outlined in a separate PAN article.

6   References

Björkman O and Demmig B (1984) Photon yield of O_2-evolution and chloroplast fluorescence characteristics at 77K among vascular plants of diverse origins. Planta 170: 489-504

Chylla RA, Garab G and Whitmarsh J (1987) Evidence for slow turnover in a fraction of Photosystem II complexes in thylakoid membranes. Biochim Biophys Acta 894: 562-571

Eilers PHC and Peeters JCH (1988) A model for the relationship between light intensity and the rate of photosynthesis in phytoplankton. Ecological Modelling 42: 199-215

Falkowski PG, Wyman K, Ley AC and Mauzerall DC (1986) Relationship of steady-state photosynthesis to fluorescence in eucaryotic algae. Biochim Biophy Acta 849: 183-192

Gilbert M, Domin A, Becker A and Wilhelm C (2000a) Estimation of primary productivity by chlorophyll a in vivo fluorescence in freshwater phytoplankton. Photosynthetica 38(1): 111-126

Gilbert M, Wilhelm C and Richter M (2000b) Bio-optical modelling of oxygen evolution using in vivo fluorescence: Comparison of measured and calculated photosynthesis/irradiance (P-I) curves in four representative phytoplankton species. J Plant Physiol 157: 307-314

Koblizek M, Kaftan D and Nedbal L (2001) On the relationship between the non-photochemical quenching of the chlorophyll fluorescence and the Photosystem II light harvesting efficiency. A repetitive flash fluorescence induction study. Photosynth Res 68: 141-152

Kolber ZS, Prasil O and Falkowski PG (1998) Measurement of variable chlorophyll fluorescence using fast repetition rate techniques: defining methodology and experimental protocols. Biochim Biophys Acta 1367: 88-106

Lavergne J and Briantais J-M (1996) Photosystem II heterogeneity. In: Ort DR and Yocum CF (ed): Oxygenic Photosynthesis: The Light Reactions. pp 265-287. Kluwer Academic Publishers, Dordrecht-Boston-London

Lavergne J and Leci E (1993) Properties of inactive PS II centers. Photosynth Res 38: 323-343

Lavergne J and Trissl H-W (1995) Theory of fluorescence induction in Photosystem II: Derivation of analytical expressions in a model including exciton-radical-pair equilibrium and restricted energy transfer between photosynthetic units. Biophys J 68: 2474-2492

Mauzerall D and Greenbaum NL (1989) The absolute size of a photosynthetic unit. Biochim Biophys Acta 974: 119-140

Melis A (1991) Dynamics of photosynthetic membrane composition and function. Biochim Biophys Acta 1058: 87-106

Nedbal L, Trtílek M and Kaftan D (1999) Flash fluorescence induction: a novel method to study regulation of Photosystem II. J Photochem Photobiol B: Biol 48: 154-157

Platt T, Gallegos CL and Harrison WG (1980) Photoinhibition of photosynthesis in natural assemblages of marine phytoplankton. J Marine Res 38: 687-701

Rappaport F, Béal D, Joliot A and Joliot P (2007) On the advantage of using green light to study fluorescence yield changes in leaves. Biochim Biophys Acta 1767: 56-67

Sakshaug E, Bricaud A, Dandonneau Y, Falkowski PG, Kiefer DA, Legendre L, Morel A, Parslow J and Takahashi M (1997) Parameters of photosynthesis: definitions, theory and interpretation of results. J Plankton Res 19 (11): 1637-1670

Samson G, Prasil O and Yaakoubd B (1999) Photochemical and thermal phases of chlorophyll a fluorescence. Photosynthetica 37(2): 163-182

Schreiber U (2004) Pulse-Amplitude (PAM) fluorometry and saturation pulse method. In: Papageorgiou G and Govindjee (eds) Chlorophyll fluorescence: A signature of Photosynthesis, pp 279-319. Kluwer Academic Publishers, Dordrecht, The Netherlands

Schreiber U, Bilger W and Neubauer C (1994) Chlorophyll fluorescence as a non-intrusive indicator for rapid assessment of in vivo photosynthesis. Ecological Studies 100: 49-70

Schreiber U, Fink R and Vidaver W (1977) Fluorescence induction in whole leaves: Differentiation between the two leaf sides and adaptation to different light regimes. Planta 133: 121-129

Schreiber U, Kühl M, Klimant I and Reising H (1996) Measurement of chlorophyll fluorescence within leaves using a modified PAM fluorometer with a fiber-optic microprobe. Photosynth Res 47: 103-109

Stirbet A, Govindjee (2011) On the relation between the Kautsky effect (chlorophyll a fluorescence induction) and Photosystem II: Basics and applications of the OJIP fluorescence transient. J Photochem Photobiol B: Biol 104: 236-257

Strasser, RJ, Tsimilli-Michael M and Srivastava A (2004) Analysis of the chlorophyll *a* fluorescence transient. In: Papageorgiou G and Govindjee (eds) Chlorophyll fluorescence: A signature of Photosynthesis, pp 321-362. Kluwer Academic Publishers, Dordrecht, The Netherlands

Vogelmann TC (1993) Plant tissue optics. Ann Rev Plant Physiol Plant Mol Biol 44: 231-251